Received: 10 November 2018 | Revised: 27 March 2019 | Accepted: 14 May 2019

DOI: 10.1002/jnr.24474

RESEARCH ARTICLE

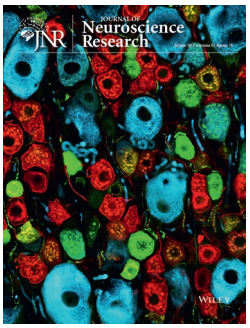

Protective roles of carbonic anhydrase 8 in Machado–Joseph Disease

Mingli Hsieh[1,2] | Benjamin Y. Hsieh[3] | Chung-Yung Ma[1] | Yi-Ting Li[1] | Chin-San Liu[4,5,6] | Che-Min Lo[1]

[1]Department of Life Science, Tunghai University, Taichung, Taiwan, Republic of China

[2]Life Science Research Center, Tunghai University, Taichung, Taiwan, Republic of China

[3]Department of Medicine, School of Medicine, National Yang-Ming University, Taipei, Taiwan, Republic of China

[4]Vascular and Genomic Research Center, Changhua Christian Hospital, Changhua, Taiwan, Republic of China

[5]Department of Neurology, Changhua Christian Hospital, Changhua, Taiwan, Republic of China

[6]Graduate Institute of Integrative Chinese and Western Medicine, China Medical University Hospital, Taichung, Taiwan, Republic of China

Correspondence
Mingli Hsieh, Department of Life Science, Tunghai University, No.1727, Sec. 4, Taiwan Boulevard, Taichung 407, Taiwan, Republic of China.
Email: mhsieh@thu.edu.tw

Funding information
Ministry of Science and Technology of the Republic of China (MOST105-2320-B-029-001-MY3; MOST106-2632-B-029-001; MOST105-2632-B-029-001; MOST104-2320-B-029-001; MOST104-2632-B-029-001; MOST103-2311-B-029-002; MOST102-2311-B-029-002; NSC101-2311-B-029-001)

Abstract

Machado–Joseph disease (MJD)/Spinocerebellar ataxia type 3 (SCA3) is an inherited neurodegenerative disease that can lead to a regression of motor coordination and muscle control in the extremities. It is known that expansion of CAG repeats encodes abnormally long polyQ in mutant ataxin-3, the disease protein. It is also noted that mutant ataxin-3 interacts with 1,4,5-trisphosphate receptor type 1 (IP3R1) and induces abnormal Ca^{2+} release. Previously, we have shown a significant increase in the expression of carbonic anhydrase VIII (CA8) in SK-N-SH-MJD78 cells, which are human neuroblastoma cells overexpressing mutant ataxin-3 with 78 glutamine repeats. In the current study, we showed the presence of significantly increased CA8 expression in MJD mouse cerebellum in either early or late disease stage, with a gradual decrease in CA8 expression as the MJD mice naturally aged. By immunofluorescence and immunoprecipitation analysis, we also found that CA8 co-localized and interacted with mutant ataxin-3 in SK-N-SH-MJD78 cells harboring overexpressed CA8 (SK-MJD78-CA8). In addition, we found that SK-MJD78-CA8 cells, as well as cerebellar granule neurons (CGNs) of MJD transgenic (Tg) mouse with overexpressed CA8, were more resistant to reactive oxygen species (ROS) stress than the control cells. Importantly, overexpression of CA8 in SK-MJD78-CA8 cells and in MJD CGNs rescued abnormal Ca^{2+} release and caused an increase in cell survival. In summary, we demonstrate the protective function of CA8 in MJD disease models and speculate that the declining expression of CA8 following an initial increased expression may be related to the late onset phenomenon of MJD.

KEYWORDS
calcium release, carbonic anhydrase 8, Machado–Joseph Disease, MJD transgenic mouse, protective function, RRID:AB_10077656, RRID:AB_2066293, RRID:AB_2129339, RRID:AB_2210209, RRID:AB_310680, RRID:AB_627809, RRID:AB_641123, RRID:CVCL_0045, RRID:CVCL_0531, RRID:IMSR_JAX:000664, RRID:IMSR_JAX:012705

1 | INTRODUCTION

Machado–Joseph disease (MJD)/spinocerebellar ataxia type 3 (SCA3) is an autosomal dominant neurodegenerative disease caused by polyglutamine expanded ataxin-3. The main symptoms of MJD include progressive ataxia, eye movement abnormalities, dysarthria, hyperreflexia, dystonia, and ophthalmoplegia (Coutinho & Andrade, 1978; Rosenberg, 1992; Soong, Cheng, Liu, & Shan, 1997). Previous neuropathological studies have detected neuronal loss in the cerebellum, midbrain, pons, medulla oblongata, and spinal cord in MJD patients (Riess, Rub, Pastore, Bauer, & Schols, 2008); and the MJD disease gene

Edited by Barrington Burnett.

All peer review communications can be found with the online version of the article.

Significance

In this study, we showed a significant increase in CA8 expression in the Purkinje cells of MJD mouse cerebellum in either early or late disease stage, as compared with its wild-type control. Additionally, we reported an interesting finding that CA8 co-localized and interacted with mutant ataxin-3. Furthermore, overexpression of CA8 in mutant MJD neuronal cells and in MJD cerebellar granule neurons rescued abnormal calcium release and caused an increase in cell survival, indicating a protective function of CA8 in MJD disease models. Our findings may provide an important information for potential therapeutic targets in the future.

was subsequently mapped to chromosome 14q32.1 (Kawaguchi et al., 1994). It was previously found that WT ataxin-3 contains 12 ~ 44 glutamine repeats with a molecular weight of approximate 42 kDa, whereas mutant ataxin-3 contains more than 52 glutamine repeats (Kawaguchi et al., 1994). WT ataxin-3 was shown to be a deubiquitinating enzyme (DUB) with a modulating function on substrate degradation through the ubiquitin–proteasome pathway (Durcan & Fon, 2013). Ataxin-3 also functions to regulate the transcriptional process and interact with numerous transcriptional regulators (Burnett & Pittman, 2005; Evert et al., 2006; McCampbell et al., 2000; Mueller et al., 2009; Shimohata et al., 2000). It has been shown that oxidative stress induced by mutant ataxin-3 could lead to mitochondrial dysfunction and cell damage (Laco, Oliveira, Paulson, & Rego, 2012). Our previous study also showed that overexpressed mutant ataxin-3 in a cell model reduced antioxidant enzyme levels and increased mitochondrial DNA damage, both indicating that mitochondrial function was impaired in MJD (Yu, Kuo, Cheng, Liu, & Hsieh, 2009).

Furthermore, the expanded polyQ stretch in the C-terminus of ataxin-3 most likely leads to pathological changes in protein conformation and binding properties. Within the cell, ataxin-3 is found to be distributed in the cytoplasm and capable of translocating to the nucleus and back (Chai, Shao, Miller, Williams, & Paulson, 2002). Furthermore, the presence of nuclear aggregations has been established as a major hallmark in MJD patients. In fact, the intracellular aggregations composed of expanded polyQ fragments and full-length ataxin-3 were observed in cerebellar neurons and ventral pons (Trottier et al., 1998). Following this discovery, the "toxic fragment hypothesis" was proposed to illustrate the proteolytic cleavage of mutant ataxin-3 in MJD disorder pathogenesis (Berke, Schmied, Brunt, Ellerby, & Paulson, 2004; Haacke et al., 2006; Takahashi et al., 2008). Additionally, mutant ataxin-3 was also found to be cleaved by calpains, a cysteine protease activated by calcium, and resulted in the formation of C-terminal ataxin-3 fragments, contributing to aggregation (Hubener et al., 2013). Several proteolytic enzymes, such as caspases and calpains, were identified to be responsible for the generation of the toxic ataxin-3 fragments (Simões, Gonçalves, Nobre, Duarte, & Pereira de Almeida, 2014). Inhibition of calpains resulted in reduced mutant ataxin-3 proteolysis, nuclear localization, aggregation, and alleviated toxicity in vitro and in vivo (Haacke, Hartl, & Breuer, 2007; Simoes et al., 2012). In addition, mutant ataxin-3 was found to bind to inositol 1,4,5-trisphosphate receptor type 1 (IP_3R1) and activated intracellular calcium release (Chen et al., 2008). Collectively, these findings suggest that the alteration of cellular calcium homeostasis plays an important role in the pathogenesis of MJD.

Carbonic anhydrase 8 (CA8) is a member of α-carbonic anhydrase family, which consists of 16 isozymes. Thirteen of the isozymes (CA1, 2, 3, 4, 5A, 5B, 6, 7, 9, 12, 13, 14, and 15) can catalyze the reversible hydration of carbon dioxide (CO_2) to bicarbonate and protons, a process that helps maintain pH balance in blood (Berthelsen, 1982). There are three additional CA isozymes called carbonic anhydrase related protein 8, 10, and 11 (CA8, 10 and 11), which lack the reversible hydration activity due to the deficiency in one or more histidine residues that are required to catalyze CO_2 hydration (Picaud et al., 2009; Sjoblom, Elleby, Wallgren, Jonsson, & Lindskog, 1996). Further, CA8 is known to be predominantly present in the Purkinje cell layer of the cerebellum in mouse and human (Aspatwar, Tolvanen, & Parkkila, 2010; Hirota, Ando, Hamada, & Mikoshiba, 2003). The expression of CA8 can also be observed in various organs, such as liver and lung (Hirota et al., 2003). Functionally, CA8 binds to inositol 1,4,5-trisphosphate receptor type 1 (IP_3R1) to decrease the affinity of IP_3 (Hirota et al., 2003).

Previous studies of CA8 mainly focused on the roles of CA8 in neurodegeneration. It was reported that the *waddles* (*wdl*) mouse, exhibiting ataxic movement and dystonia, harbors a 19-bp deletion in *ca8* gene (Jiao et al., 2005). Furthermore, two homozygous point mutations in *CA8* gene, S100P and G162R, were reported in patients with cerebellar ataxia and cerebellar atrophy in Iraqi families (Kaya et al., 2011; Turkmen et al., 2009). Previous studies from our laboratory also demonstrated that knockdown of CA8 in zebrafish larvae resulted in abnormal phenotypes, defective locomotion, and neuronal cell death (Huang et al., 2014). In addition, we showed a significant decrease in CA8 mRNA and protein expression in cybrid cells containing MERRF A8344G mutation. Myoclonus epilepsy associated with ragged-red fibers (MERRF) syndrome is a mitochondrial disease with pathological features of ataxia and myoclonus. Moreover, overexpression of CA8 has been identified to play a protective function in MERRF cybrids (Wang et al., 2014). These findings support that CA8 plays an important role in neuron function and cerebellum development. Additionally, our previous results have revealed that CA8 was significantly increased in human neuroblastoma cells harboring mutant ataxin-3 as compared with cells containing WT ataxin-3 (Hsieh et al., 2013). However, the mechanisms underlying these observations remain to be addressed.

In this study, we hope to further study the expression and function of CA8 in MJD cellular and animal models. A MJD Tg mouse model was previously established by Cemal and colleagues (Cemal et al., 2002). The MJD Tg mice, harboring two copies of human MJD1 gene with 84 CAG repeats, demonstrated a mild and slowly progressive cerebellar deficit. As the disease progressed in the mice, hypotonia, motor and sensory loss emerged. Neuronal intranuclear inclusion (NII) formation and neuronal cell loss were prominent in the

pontine and in the cerebellum (Cemal et al., 2002). Therefore, the MJD Tg mice could be used as a valuable resource for the detailed analysis of the roles of CA8 in the neurodegenerative processes underlying MJD pathogenesis. Using MJD Tg mice and the WT control along with two cellular models created in our laboratory, we aimed to understand the regulation and functions of CA8 in the presence of mutant ataxin-3 in vitro and in vivo.

2 | METHODS

2.1 | Animals

C57BL/6J MJD mice expressing two copies of human ataxin-3 gene with 84 CAG repeats (Cemal et al., 2002) (IMSR Cat# JAX:012705, RRID:IMSR_JAX:012705) and their WT littermates were purchased from Jackson's laboratory (Bar Harbor, ME). All mice were of C57BL/6J background (IMSR Cat# JAX:000664, RRID:IMSR_JAX:000664), and the generation of transgenic mice was achieved as described (Chen et al., 2008). The identities of the MJD transgenic mice were confirmed by genomic PCR from the mouse tail DNA (Chen et al., 2008). The primers used were: 5′-CCAGTGACTACTTTGATTCG-3′ and 5′-TGGCCTTTCACATGGATGTGAA-3′ for human MJD1 gene; 5′-CATCACCATCTTCCAGGAGC-3′ and 5′-ATGCCAGTGAGCTTCCCGTTC-3′ for mouse GAPDH (Glyceraldehyde-3-phosphate-dehydrogenase). Animals were maintained on a 12-hr light/dark cycle with free access to food and water. Both male and female mice, without regard to sex, were utilized for all experiments. The mice were sacrificed under Zoletil 50 and all the efforts were made to minimize suffering. All the procedures involving mice in this research were approved by the Institutional Animal Care and Use Committee of Tunghai University (#102-24; 103-19; 104-22).

2.2 | Cell lines and antibodies

Human neuroblastoma cell line SK-N-SH (ATCC Cat# HTB-11, RRID:CVCL_0531) was provided by Dr. Shin-Lan Hsu (Taichung Veterans General Hospital, Taiwan) and human embryonic kidney cell line HEK293 (ATCC Cat# CRL-1573, RRID:CVCL_0045) was provided by Dr. Hsi-Chi Lu (Tunghai University, Taiwan). All materials for cell culture were obtained from Gibco Life Technologies (Gaithersburg, MD). Mouse monoclonal antibody against ataxin-3 (Millipore Cat# MAB5360, RRID:AB_2129339) and rabbit polyclonal antibody against IP_3R1 (Millipore Cat# 07-514, RRID:AB_310680) were from Merck Millipore (Billerica, MA). Mouse monoclonal antibodies against HA (Santa Cruz Biotechnology Cat# sc-7392, RRID:AB_627809) and GFP (Santa Cruz Biotechnology Cat# sc-8334, RRID:AB_641123) were obtained from Santa Cruz Biotechnology (Santa Cruz, CA). Rabbit polyclonal antibody against CA8 (Santa Cruz Biotechnology Cat# sc-67330, RRID:AB_2066293) was obtained from Santa Cruz Biotechnology (Santa Cruz, CA). Mouse monoclonal antibodies against β-actin (Novus Cat# NB600-501, RRID:AB_10077656) and α-tubulin (Novus Cat# NB100-690, RRID:AB_2210209) were obtained from Novus Biologicals (Littleton, CO).

2.3 | Isolation of total RNA and RT-PCR

Mice were anesthetized with Zoletil 50 and sacrificed by decapitation. Brains were removed for immediate dissection. Total RNA was extracted from the cerebellum of mice (n = 6/group from both sexes) using TRIzol® reagent from Life Technologies. Semi-quantitative RT-PCR (reverse transcription PCR) was performed. Four microgram of total RNA was reverse transcribed into cDNA in a final volume of 20 μl with 50 pmol oligo-dT primer, 0.5 mM dNTP and 200 units of MMLV (Moloney murine leukemia virus) reverse transcriptase (Life Technologies) for 50 min at 37°C and 15 min at 70°C. The primers used were: 5′-TCCTGATGCTAATGGGGAATACCAG-3′ and 5′-CTAAGAGGCTGAGTGGGCCGAAAG-3′ for CA8; 5′-CCATGACAACTTTGGCATTG-3′ and 5′-CCTGCTTCACCACCTTCTTG-3′ for GAPDH (Glyceraldehyde-3-phosphate-dehydrogenase). The PCR consisted of varying cycles with denaturation at 94°C for 30 s, annealing at 57°C for 30 s, and elongation at 72°C for 30 s. The PCR-amplified DNA products were electrophoretically separated on 1% of agarose gels. In order to compare the amplified products semi-quantitatively, signal quantification was performed using a densitometric scanner (Image J). We confirmed that the amounts of PCR products were at a linear range after 22 cycles of PCR amplification.

2.4 | Preparation of lysate for SDS/PAGE

Mice were anesthetized with Zoletil 50 and sacrificed by decapitation. Brains were removed for immediate dissection (n = 5–8/group from both sexes). The cerebellum tissues or cells were washed twice with PBS, resuspended in 500 μl of lysis buffer (15% of glycerol, 1 mM of sodium EDTA, 1 mM of sodium EGTA,1 mM of DTT, 40 μg/ml of leupeptin, 20 μg/ml of pepstain, 1 mM of PMSF, and 0.5% of Triton X-100 in PBS) and then sonicated on ice for 15 min. The resulting lysate was centrifuged at 13,000 rpm for 30 min at 4°C. The supernatant was collected and the protein concentration was determined using the Bio-Rad protein assay.

2.5 | Western blotting

The cell lysates containing 10–30 μg of protein were loaded by 10% of sodium dodecyl sulfate (SDS) polyacrylamide gels. The resolved proteins were electrophoretically transferred on to 0.2 μm PVDF membranes. After blocking the membrane with 5% (w/v) non-fat milk powder in TTBS (10 mM of Tris/HCl (pH 7.5), 150 mM of NaCl, and 0.1% of Tween 20) buffer for 1 hr at room temperature, the antibody binding reaction was performed in the same buffer at 4°C overnight or at room temperature for 1 hr for primary antibodies and at room temperature for 1 hr for secondary antibodies to couple to HRP (horseradish peroxidase)-conjugated anti-(goat IgG) antibody. Pre-stained high molecular mass markers were included. Signals were captured by the enhanced chemiluminescent (Millipore). Protein bands were quantified by densitometry, and protein loading was normalized with β-actin or α-tubulin. For quantification of proteins, the amount of proteins loaded on to the gel was optimized, and

multiple exposures were performed to ensure that the signals were within the linear response range.

2.6 | Plasmid construction

Plasmid MJD26-GFP containing full-length MJD with 26 glutamines, plasmid MJD78-GFP containing full-length MJD with 78 glutamines and plasmid tMJD78-GFP lacking N-terminus of MJD (with amino acids 56–279 deleted) were constructed previously (Chang, Tien, Chen, Nukina, & Hsieh, 2009). Plasmid pcDNA3.1 containing full-length MJD with 78 glutamines was a gift from Dr. Henry Paulson. A lentivirus transfer vector containing full-length CA8 with myc tagged (pLKOAS3w.puro.CA8-myc) was constructed by Tang-Hao Chi (unpublished data). The recombinant DNA sequence was confirmed by DNA sequencing. The lentiviral eGFP expression vectors of control (pLKOAS7w.eGFP.puro), shRNA expression vectors of sh-Ctrl (pLKO.1-shLuc) and sh-CA8 (TRCN000155916) were purchased from the National RNAi Core Facility (Institute of Molecular Biology, Academia Sinica, Taipei, Taiwan).

2.7 | Cell culture and selection of stable cells

Human neuroblastoma cell line was maintained in a medium containing Dulbecco's modified Eagle's medium (DMEM) supplemented with 1% of non-essential amino acid, 100 units/ml of penicillin, 100 μg/ml of streptomycin, 2 mM of L-glutamine, 10% of fetal bovine serum (FBS), and 100 μg/ml of pyruvate. SK-N-SH cells were transfected with pCDNA3-HAMJD78 and a stable cell line (SK-MJD78) was selected in a culture medium supplemented with G418 (neomycin sulfate, 500 μg/ml) (Wen et al., 2003). Viruses carrying recombinant pLKOAS3w-CA8-myc.puro and pLKOAS7w.eGFP.puro were generated by the National RNAi Core Facility in Academia Sinica. Infection of the modified virus for stable expression of CA8 was performed according to the instructions provided by the National RNAi Core Facility. SK-MJD78 cells infected with recombinant lentivirus were selected using 0.7 μg/ml puromycin (Sigma). Expression of CA8 proteins was determined by Western blot analysis using an anti-CA8 antibody. Expression of eGFP proteins was determined by Western blot analysis using an anti-GFP antibody. After 5 days of selection, the surviving cells were grown in a medium containing 0.7 μg/ml of puromycin. Stable cells were collected after 10–15 days. Human embryonic kidney (HEK293) cell line was maintained in a medium (MEM) supplemented with 1% of non-essential amino acid, 100 units/ml of penicillin, 100 μg/ml of streptomycin, 2 mM of L-glutamine, 10% of fetal bovine serum (FBS), and 100 μg/ml of pyruvate. Cells were transfected using Polyjet reagent (SignaGen) following the manufacturer's instructions. Cells were transfected with 1 μg of MJD26-eGFP, MJD78-eGFP, or tMJD78-GFP. Eighteen hours after transfection, cells were selected in a culture medium supplemented with 500 μg/ml G418 (Life Technologies). Expression of GFP proteins was determined by Western blot analysis using an anti-GFP antibody. After 14 days of selection, the surviving cells were diluted to a density of 10 cells/ml and grown in a medium containing 500 μg/ml of G418. Stable cells were collected after 14–20 days. For all experiments, cells were placed in a medium lacking puromycin and G418.

2.8 | Luciferase activity

A luciferase reporter plasmid containing the full-length of CA8 promoter was constructed previously (Lo, Ma, Wei, Hsieh, & Hsieh, 2018). The construct was co-transfected into HEK293 cell lines (HEK293-MJD26, HEK293-MJD78 and HEK293-tMJD78) along with a β-galactosidase (β-gal) vector. After 48 hr, luciferase activity was measured and normalized to β-galactosidase levels. Promoter activity was determined by measuring relative luciferase activity in the transfected cells using a luciferase reporter kit (Promega, Madison, WI). In these experiments, all the data were normalized to β-galactosidase activity.

2.9 | Immunohistochemistry

The cerebellum tissues were isolated from MJD Tg mice and age-matched WT mice at ages of 3 weeks, 26 weeks, or 52 weeks after sacrificed with Zoletil 50 (n = 5–8/group from both sexes), and fixed at 4°C in 4% of paraformaldehyde (PA) in PBS overnight. The fixed cerebellum tissues were washed with PBS, and incubated in 10% of sucrose solution at 4°C for 1 hr; in 20% of sucrose solution at 4°C for 2 hr; and in 30% of sucrose solution at 4°C overnight. The cerebellum tissues were frozen by OCT compound (Tissue Freezing Medium) and 10 μm sections were cut using a cryostat (LEICA CM3050S) at −20°C. After washing with PBS, cerebellum tissues were blocked using 10% of fetal bovine serum (FBS) in PBS for 1 hr at room temperature. The samples were incubated with the primary antibody solution at 4°C overnight (1:200 anti-CA8). Endogenous peroxidases were blocked using 30% of hydrogen peroxide (H_2O_2) for 30 min at room temperature. After washing with PBS for three times, the samples were incubated with secondary antibodies for 2 hr at room temperature (1:200 dilution, HRP conjugated goat anti-rabbit IgG). After washing with PBS, the diaminobenzidine substrate (DAB; KOMA) was added, and the reaction was stopped in PBS after the desired degree of straining was reached. Slides were counterstained with hematoxylin (Merck). Finally, slides were mounted by permount mounting medium (Fisher Scientific). The immunohistochemistry results were scored by taking into account the intensity of the staining. Each slide was examined and scored blindly by 15 examiners who assigned a score of 0 (no staining), 1 (slightly staining), 2 (moderately staining), or 3 (most intense staining) within Purkinje cell layers, then the averages of the scores were recorded for comparison and statistical analysis.

2.10 | Immunofluorescence

WT and MJD Tg mice at age of 52 weeks (n = 3/group) were anesthetized with Zoletil 50 and perfused intracardially with ice-cold 4% of paraformaldehyde in phosphate buffered saline (PBS). Brains were removed and postfixed overnight. The samples were cryoprotected in graded sucrose over a 5 day period and then embedded

and frozen in Tissue-Tek O.C.T. Compound (Sakura Finetek USA, Inc. Torrance, CA) and stored at −80°C until use. The tissues were cut at 10 μm sections by a cryostat (LEICA CM3050S) at −20°C. Cells were seeded on glass coverslips at 3×10^5 cells/well in six-well tissue culture plates and incubated for 48 hr at a 37°C in a 5% of CO2 incubator. Cells were then washed three times with PBS (pH 7.4), fixed and permeabilized with 4% of paraformaldehyde (PA) in PBS for 20 min at room temperature. After washing with PBS, cells and tissues were blocked using 10% of fetal bovine serum (FBS) in PBS for 1 hr at room temperature. The samples were incubated with the primary antibody solution at 4°C overnight (anti-ATXN3, 1:1,000, 1:200 anti-CA8, 1:100 anti-GFP, 1:200 anti-HA, and 1:100 anti-myc). After washing with PBS for three times, the samples were incubated with secondary antibodies and propidium iodide (PI) for 2 hr at room temperature (1:500 PI, 1:200 anti-mouse IgG FITC, and anti-rabbit-IgG DyLight 649). Finally, cells and tissues were washed three times and mounted. The images were recorded on Zeiss LSM 510 confocal microscope.

2.11 | Immunoprecipitation

Cells were solubilized in lysis buffer (50 mM of Tris-HCl, pH 7.9, 150 mM of NaCl, 1% of NP-40, 1X protein inhibitor cocktail, 10% of glycerol, 1.5 Mm of $MgCl_2$, 1mM of EGTA, 1mM of EDTA) and lysates were cleared by centrifugation. Equal amounts of total proteins were incubated with monoclonal anti-myc or polyclonal anti-CA8 for 1 hr, and then incubated with Protein A agarose beads overnight. The beads were pelleted by centrifugation and washed with washing buffer (50 mM of Tris-HCl, pH 7.9, 150 mM of NaCl, 1%of NP-40, 10% of glycerol, 1.5 Mm of $MgCl_2$, 1mM of EGTA, 1mM of EDTA). The immunopellets were resuspended in SDS-PAGE sample buffer and subjected to electrophoresis and Western blot analysis.

2.12 | Mouse cerebellar granule neuron (CGN) isolation and treatment

C57BL/6J WT and MJD mice (postnatal day 5–7) (n = 3/group) were anesthetized on ice for a few minutes before decapitation, then the crumbed meninges and cerebellum tissue were carefully removed using fine tweezers. The cerebellum tissue was then incubated for 10 min in 1 ml of dissociation solution containing 0.25% of trypsin and 1 mM of EDTA at 37°C, pipetted with P1000 pipet every 5 min, centrifuged at 1,000 rpm for 5 min, and then the supernatant was removed. 10 μl of 10 mg/ml of DNase I (Sigma) was added to the pellet, after briefly tipping the tube, 1 ml of DMEM containing 20% of FBS was added into the tube. The mixture was centrifuged at 1,000 rpm for 5 min, and then the supernatant was removed. Four millilitrer of 20% of FBS DMEM was added in to the pellet (cerebellar granule neurons). After cell counting, we seeded 1×10^6 CGNs into 3 cm dishes for the following experiments. For lentivirus infection, 5×10^5 of CGNs were seeded in 3 cm dishes with 20% of FBS DMEM for 24 hr. One day after, culture media were replaced by 20% of FBS DMEM containing 8 μg/ml of polybrene. According to the virus titer, we added the appropriate amounts of lentivirus carrying recombinant pLKOAS3w-CA8-myc-puro, CA8 shRNA (pLKO.1-shCA8, TRCN000155916), or control vector (pLKOAS7w.eGFP.puro and pLKO.1-shLuc) (M.O.I = 3) into CGNs for 12 hr infection. After lentivirus infection, the infection medium was replaced by 20% of FBS DMEM, selected by 1 μg/ml of puromycin (Sigma) for 3 days and then incubated until cells were placed in a medium lacking puromycin before the experiments.

2.13 | Cell viability

SK-N-SH cell lines were seeded at the density of 1.3×10^5 cells/well and CGNs were seeded at the density of 2×10^4 cells/well in a 96-well tissue culture plate incubated for 24 hr in a 37°C, 5% CO2 incubator. One day after seeding, cells were incubated for 30 min in a fresh medium containing 20 μM or 3μM of H_2O_2 for SK-N-SH and CGNs, respectively. For treatments with various agents, SK-N-SH cells were treated with 5 μM of A23187, 20 μM of calpeptin, or 10μM of BAPTA-AM for 10 min before being treated with H_2O_2. CGNs were treated with 10 μM of A23187, 10 μM of calpeptin, or 5 μM of BAPTA-AM for 2 hr and 30 min before being treated with H_2O_2. Cell viability was determined with the 3-(4,5-dimethylthiazol-2-yl)-2,5-diphenyltetrazolium bromide (MTT) assay (Sigma). Then MTT (5 mg/ml) were added to each well and the mixture was incubated at 37°C for 4 hr. To dissolve formazan crystals, the culture medium was then replaced with an equal volume of DMSO. After the mixture was shaken at room temperature (RT) for 10 min, absorbance of each well was determined at 570 nm using a microplate reader. Results were expressed as the percentage of controls.

2.14 | Measurement of intracellular Ca^{2+}

SK-N-SH cell lines were seeded at the density of 1.3×10^5 cells/well and mouse CGNs were seeded at the density of 2×10^4 cells/well in a 96-well tissue culture plate incubated for 24 hr in a 37°C, 5% CO_2 incubator. After 24 hr, cells were washed by HEPES buffer with Ca^{2+}, and loaded with 2.5 μM Fura-4AM in the HEPES buffer with Ca^{2+}. After 45 min, cells were washed by the HEPES buffer without Ca^{2+}, and incubated for 30 min. Finally, cytosolic Ca^{2+} signal in cells was assessed in response to 0.1mM of ATP. Fura-4AM fluorescence was recorded continuously at 37°C in a spectrofluorometer at the excitation wavelength of 494 nm and an emission wavelength of 516 nm.

2.15 | Statistics

Statistical analysis was performed using R software (version 3.5.3). All data are expressed as box plots. When two groups were compared, significant differences were analyzed using the Student's t test. In Figure 2 and Figures 12 through 14, a two-way ANOVA was used to address the two factor design of mice type/time and mice type/treatment, respectively. Assumptions of normality of residuals were checked with Shapiro–Wilk test. Multiple pairwise comparisons were assessed by post hoc Tukey's HSD. Figure legend indicates which test was used for each corresponding experiment. Differences were considered statistically significant if the p value was less than 0.05.

3 | RESULTS

3.1 | Protein expression of CA8 in a MJD Tg mouse model

We have previously found an increased expression of CA8 in human neuroblastoma cells containing mutant ataxin-3, as compared with that in control human neuroblastoma cells containing WT ataxin-3 (Hsieh et al., 2013). Therefore, we were interested in evaluating the expression levels of CA8 in the cerebellum tissue of MJD Tg mice. Semi-quantitative RT-PCR and Western blot analysis were performed to determine the CA8 expression levels. Our results showed that the expression of mRNA and protein levels in the Tg mice at age of 3 weeks or 52 weeks were both moderately higher than those of the WT mice (Figure 1) (p = 0.013, Figure 1a; p = 0.002, Figure 1b; p = 0.007, Figure 1c; p < 0.001, Figure 1d). However, it is noted that the differences may not be clearly visible in the corresponding images. Given the fact that CA8 is predominantly present in the Purkinje cell layer of mouse cerebellum (Aspatwar et al., 2010) but the total RNAs and proteins were isolated from different cell types in the cerebellum, the expression of CA8 in MJD Tg mice may need to be further verified.

3.2 | Immunohistochemistry of CA8 expression in WT and MJD Tg mice

To further confirm the increased expression of CA8 in the Purkinje cell layer of MJD Tg mouse, we used immunohistochemical staining to examine the expression patterns of CA8. As shown in Figure 2a–d, CA8 was detected in Purkinje cells and more intense stains were observed in MJD Tg mice of 3 weeks and 52 weeks, as compared with those of the control WT mice. To quantify the results, immunohistochemical scoring systems, which take into account the intensity of staining (Tsai et al., 2014), was used for the analysis. Quantitative analysis demonstrated that a significant increase in CA8 was observed in MJD Tg mice of 3 weeks (p < 0.001), 26 weeks (p = 0.021) and 52 weeks (p = 0.027) as compared with those in age-matched WT mice (Figure 2e). It is worth noting that as the MJD Tg mice naturally aged, the expression level of CA8 gradually decreased (p < 0.001).

3.3 | Increased CA8 promoter activity in HEK293-MJD78 cells

To establish a set of MJD disease cellular model, we transfected three constructs, containing WT ataxin-3 (MJD26), mutant ataxin-3

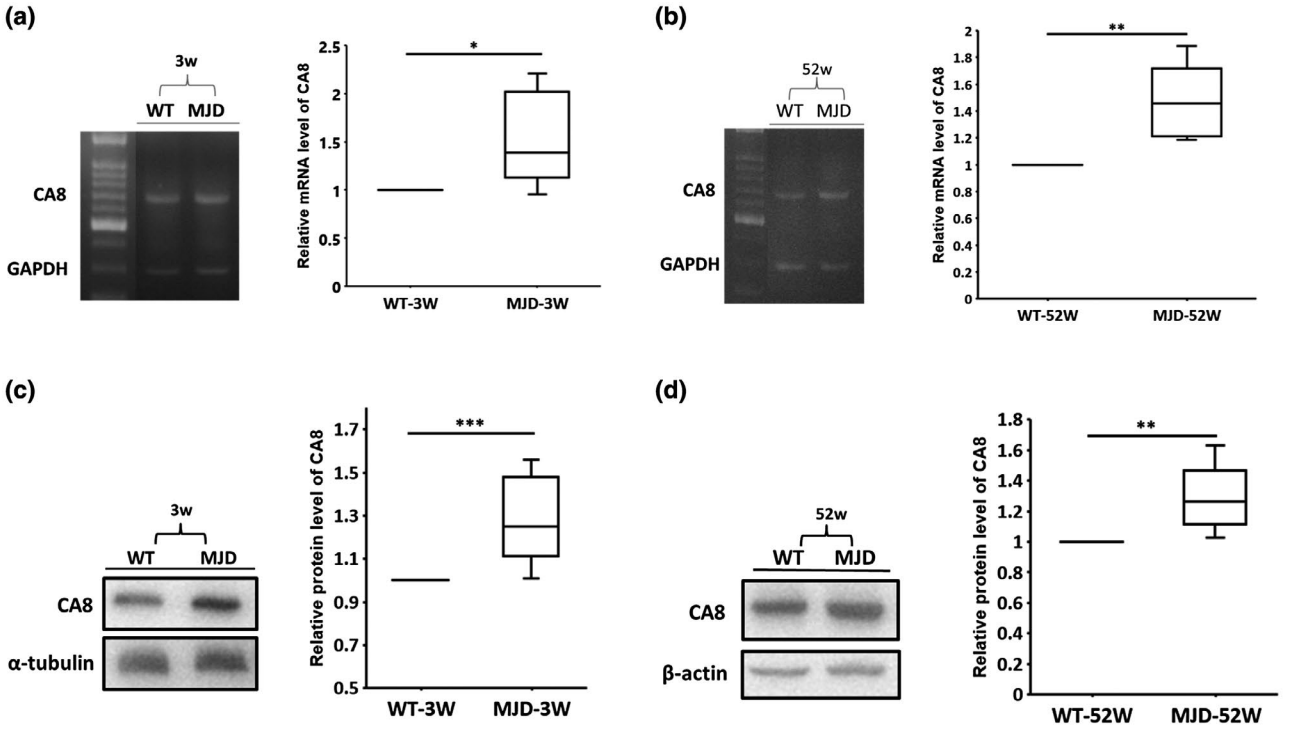

FIGURE 1 CA8 mRNA and protein analysis in the WT and MJD Tg mice. (a and b) The mRNA levels were higher in MJD Tg mice of 3 weeks (a) and 52 weeks (b) than those of WT. Total RNA from the cerebellum of MJD Tg mice, as well as the age-matched WT control, was analyzed. RT-PCR was performed using GAPDH primers as a control. The quantified values were presented as fold change compared to WT from four independent experiments. n = 6 for each set of animals. *p < 0.05, **p < 0.01. (Student's t test) (c and d) Western blot analysis of CA8 expression in MJD Tg mice of 3 weeks (c) and 52 weeks (d). CA8 protein level in MJD Tg mouse is higher than that of the WT control. Total protein from the cerebellum of MJD Tg mice, as well as their age-matched WT control, was analyzed. Expression of α-tubulin and β-actin was examined as a quantity control. Data were presented as fold change compared to WT from five independent experiments. n = 8 for MJD Tg mice of 52 weeks and the age-matched WT control; n = 5 for MJD Tg mice of 3 weeks and the age-matched WT control. **p < 0.01, ***p < 0.001. (Student's t test) [Color figure can be viewed at wileyonlinelibrary.com]

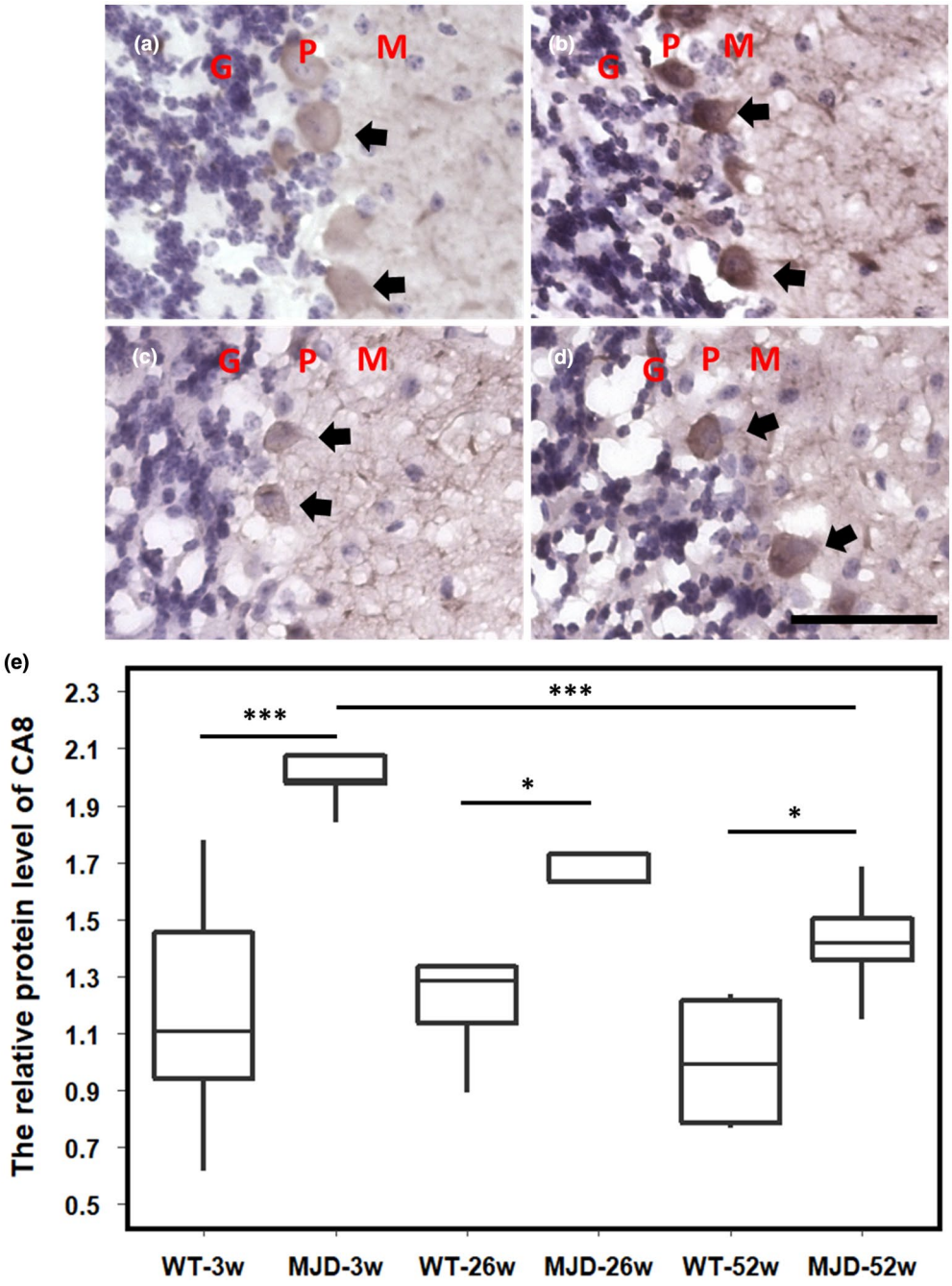

FIGURE 2 Immunohistochemistry of CA8 expression in the WT and MJD Tg mice. CA8 was detected in Purkinje cells by immunohistochemistry (arrow sign) and the more intense staining was observed in MJD Tg mice of 3 weeks and 52 weeks (b and d), as compared with the control WT (a and c). P: Purkinje cell layer, G: Granular cell layer, M: Molecular cell layer. Scale bar represents 100 μm. (e) The quantitative analysis indicated a significant increased CA8 expression in Purkinje cells of MJD mice of 3 weeks (3w), 26 weeks (26w), or 52 weeks (52w), as compared with its WT control (n = 5-8/group). Data were presented from five independent experiments. $^{*}p < 0.05$, $^{***}p < 0.001$. (Two-way ANOVA followed by Tukey's HSD test)

(MJD78), and N-terminal truncated mutant ataxin-3 (tMJD78), respectively, into HEK293 cells (Chang et al., 2009) (Figure 3a). Stable clones designated HEK293-MJD26, HEK293-MJD78, and HEK293-tMJD78 were established by proper antibiotic selection. As shown in Figure 3b, the expression of ataxin-3 was confirmed in all three stable cell lines. Consistent with what was observed in MJD Tg mice (Figure 1c,d), the expression of CA8 was increased in HEK293 cells containing mutant ataxin-3 and truncated mutant ataxin-3, as compared with that in cells harboring WT ataxin-3. Because the increased mRNA and protein levels of CA8 may indicate altered transcription regulation, we assayed the promoter activity of CA8 in HEK293 stable cells with WT or mutant ataxin-3. We transfected a luciferase reporter plasmid containing the full-length of CA8 promoter (Lo et al., 2018) into HEK293-MJD26, HEK293-MJD78, and HEK293-tMJD78 cells along with a β-gal vector

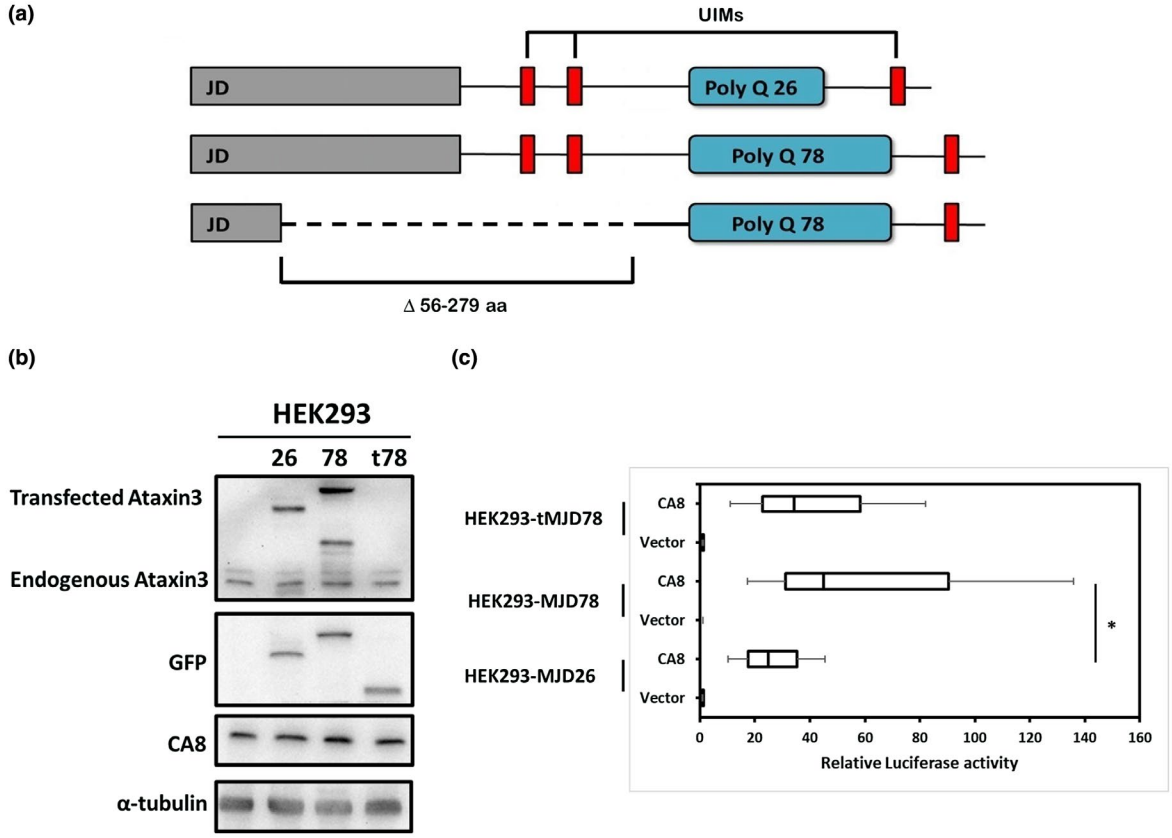

FIGURE 3 The ectopic expression of ataxin-3 and CA8 promoter activity in HEK293 cells. (a) A schematic diagram to illustrate three constructs containing ataxin-3 gene with 26 CAG repeats, 78 CAG repeats and N-terminal truncated 78 CAG repeats. JD represents Josephin domain. UIMs are ubiquitin-interacting motifs. (b) Western blot analysis of endogenous and exogenous ataxin-3 expression in HEK293 cells. All the three plasmids are GFP-tagged. Western blot analysis was performed using antibodies against ataxin-3, CA8 or GFP. Expression of α-tubulin was examined as a loading control. (c) Increased CA8 promoter activity in HEK293 cells harboring mutant ataxin 3. A construct containing the full-length of CA8 promoter region cloned into luciferase vector was co-transfected into HEK293 cell lines (HEK293-MJD26, HEK293-MJD78, and HEK293-tMJD78) along with a β-gal vector. The luciferase activity of HEK293-MJD78 was higher than HEK293-MJD26. Relative luciferase activity was calculated with respect to cells transfected with vector alone. Data were presented from three independent experiments, each performed in duplicate. $^*p < 0.05$. (Student's *t* test) [Color figure can be viewed at wileyonlinelibrary.com]

as a transfection control. As shown in Figure 3c, the luciferase activity of HEK293-MJD78 cells was clearly higher than that of HEK293-MJD26 cells ($p = 0.045$), suggesting that CA8 is upregulated at the transcription level in the presence of mutant ataxin-3. However, we did not observed a significant increase in CA8 transcripts in HEK293-tMJD78 cells, as compared with that of HEK293-MJD26 cells.

3.4 | CA8 is co-localized with mutant ataxin-3 in SK-MJD78-CA8 and in HEK293-MJD78 cells

Our previous study demonstrated that a higher mRNA expression of CA8 in SK-MJD78 cells than that in SK-MJD26 cells (Hsieh et al., 2013). However, due to the lack of endogenous CA8 protein detected by antibodies against CA8 in SK-MJD78 cells (Figure 4), viruses carrying recombinant plasmid pLKOAS3w.puro.CA8-myc (a lentivirus transfer vector containing full-length CA8) and pLKOAS7w.eGFP.puro (control virus) were used to infect SK-MJD78 cells. Stable clones, designated SK-MJD78-eGFP (SK-MJD78 cells infected with virus carrying pLKOAS7w.eGFP.puro) and SK-MJD78-CA8 (SK-MJD78 cells infected with virus carrying pLKOAS3w.puro.CA8-myc), were obtained after proper antibiotic selection. As shown in Figure 4, the ectopic expression of CA8 was confirmed in SK-MJD78-CA8 cells, with a positive control signal of CA8 from HOS-CA8 cells (Figure 4a), which was made previously by overexpressing CA8 in human osteosarcoma cells HOS (Wang et al., 2016). In addition, GFP expression was clearly detected in SK-MJD78-eGFP with HOS-eGFP as a positive control (Figure 4b). WT and mutant ataxin-3 expression was also validated in those four cell lines (Figure 4c). Next, we used immunofluorescence to examine the distributions of ataxin-3 and CA8 in SK-MJD78 cells with stably overexpressed CA8 (SK-MJD78-CA8) or in HEK293 cells with stably overexpressed WT full-length ataxin-3 (HEK293-MJD26), mutant full-length ataxin-3 (HEK293-MJD78), or mutant truncated ataxin-3 (HEK293-tMJD78). As shown in Figure 5a,b, both CA8 and mutant ataxin-3 were mainly distributed in the cytoplasm and

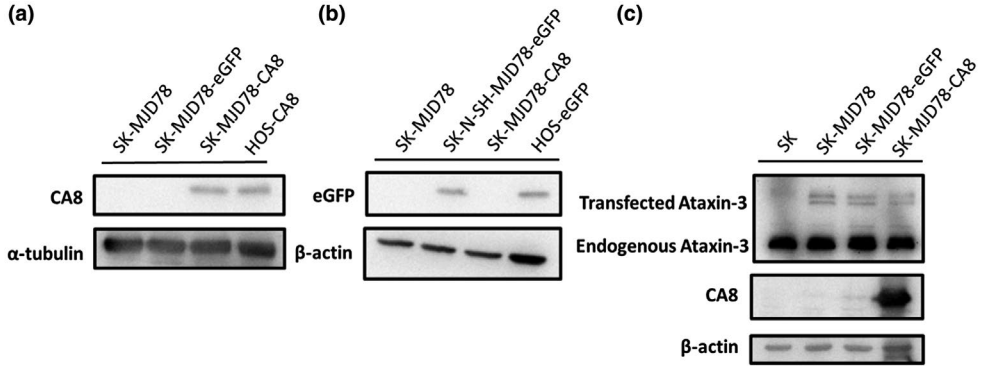

FIGURE 4 Protein expression of CA8 and ataxin-3 in SK-MJD78 cells with and without CA8 expression. (a) Western blot analysis of CA8 in SK-MJD78 cells with overexpression of CA8 (SK-MJD78-CA8) or eGFP (SK-MJD78-eGFP). HOS-CA8 was used as a positive control for the signal of CA8. (b) Western blot analysis of eGFP in SK-MJD78 cells harboring overexpressed CA8 or eGFP. HOS-eGFP was used as a positive control for the signal of eGFP. (c) Western blot analysis of ataxin-3 in SK-N-SH, SK-MJD78, SK-MJD78-eGFP, and SK-MJD78-CA8 cells. Endogenous ataxin-3 (~42 kDa) and mutant ataxin-3 (~60 kDa) were detected by antibodies against ataxin-3. Expression of α-tubulin and β-actin was examined for a loading control

co-localized together in these two MJD cellular models. It is further noted that there was no difference in the distribution of CA8 among the three HEK293 cell lines, suggesting that the cellular distribution of CA8 is not altered by the presence or absence of mutant ataxin-3.

3.5 | CA8 interacts with mutant ataxin-3 IN MJD cellular models

It is known that mutant ataxin-3 interacts with inositol 1,4,5-trisphosphate receptor type 1 (IP_3R1) (Chen et al., 2008). In addition, CA8 interacts with IP_3R1 and acts as an IP_3R1-binding protein (Hirota et al., 2003). Since our results showed that CA8 and ataxin-3 were co-localized in SK-MJD78-CA8 and HEK293-derived MJD cell lines, we next examined the possible interaction between CA8 and ataxin-3 by immunoprecipitation. Interestingly, our analysis revealed a protein–protein interaction between CA8 and ataxin-3 in SK-MJD78-CA8 cells (Figure 6a,b). Moreover, our results showed that the interaction existed only between CA8 and mutant ataxin-3 in HEK293-MJD78 cells, not in HEK293-MJD26 (Figure 6c,d). Meanwhile, we tried to determine whether the endogenous CA8 interacts with mutant ataxin-3 using cerebellum extract from MJD Tg mice. Unfortunately, we failed to detect the interaction between CA8 and mutant ataxin-3 using antibody against CA8 by immunoprecipitation (Figure 7a,b). Nevertheless, in an attempt to analyze their distributions by immunofluorescence, we found that CA8 and mutant ataxin-3 were partially co-localized in Purkinje cells of MJD Tg mice (Figure 7c). Taken together, these observations suggest that the interaction between endogenous CA8 and mutant ataxin-3 in MJD Tg mice may be relatively weak to non-detectable under our experimental conditions.

3.6 | Overexpression of CA8 desensitizes SK-MJD78 cells to oxidative stress

It was noted that overexpression of CA8 in MERFF mutant cells protected cells from apoptosis upon pro-apoptotic treatment (Wang et al., 2014). Therefore, we attempted to understand whether CA8 plays a protective role in SK-MJD78 cells by examining cell survival under oxidative stress. As shown in Figure 8a, SK-MJD78 cells were more susceptible to oxidative stress than the parental SK-N-SH cells ($p < 0.001$), which is consistent with our previous report (Wen et al., 2003). Furthermore, overexpression of CA8 in SK-MJD78-CA8 cells significantly desensitized cells to H_2O_2 treatment as compared with that in SK-MJD78-eGFP cells (Figure 8b) ($p = 0.012$), supporting a protective role of CA8 in the MJD disease cellular model.

Given that the overexpression of CA8 reduced cell death in the neuronal cells, we investigated the protective effects of CA8 in MJD cerebellar granule neurons (CGNs). To examine the effects of CA8 on granule neuron survival, CGNs were isolated from WT and MJD Tg mice, and then infected with viruses carrying overexpressed CA8, CA8-shRNA, control pLKO.1-shLUC, and control pLKOAS7w.eGFP.puro, respectively. As shown in Figure 9a, the expression level of CA8 was significantly increased in CGNs with CA8 overexpression, and moderately decreased in CGNs with CA8 knockdown; as compared with that of the individual control. The infected CGNs were further treated with 3 μM of H_2O_2 and cell viability was measured by MTT assay to study the effects of CA8. The results showed no significant difference of cell viability between WT CGNs with overexpression and downregulation of CA8 (Figure 9b,c). However, overexpression of CA8 in MJD CGNs resulted in an increase in the cell survival as compared with that of the control cells (Figure 9e) ($p < 0.001$). These findings suggest that upregulation of CA8 has protective effects not only on neuronal cell lines but also on primary CGNs from MJD Tg mice.

3.7 | CA8 rescues abnormal Ca^{2+} release in SK-MJD78 cells and in MJD CGNs

Previous evidence showed that neuronal Ca^{2+} signaling was abnormally increased in the pathogenesis of SCA3 (Bezprozvanny, 2009). Mutant ataxin-3 was also found to interact with IP_3R1 and activate

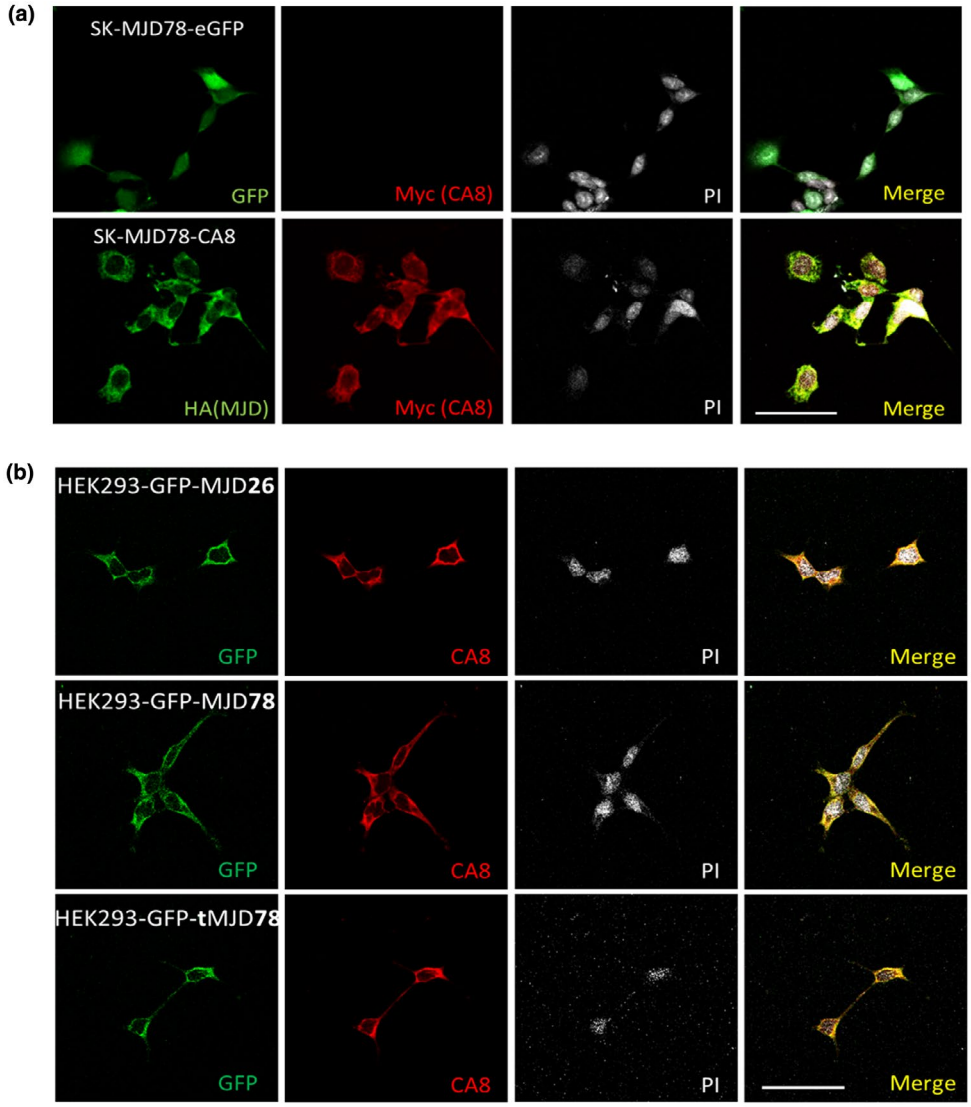

FIGURE 5 CA8 was co-localized with mutant ataxin-3 in SK-MJD78 cells with overexpressed CA8 (SK-MJD78-CA8) and HEK293 MJD cell lines. (a) SK-MJD78-CA8 cells, stably expressing HA-tagged mutant ataxin-3 and myc-tagged CA8, and SK-MJD78-eGFP cells, stably expressing HA-tagged mutant ataxin-3 and GFP, were seeded on coverslips and analyzed by immunofluorescence using anti-HA-specific, anti-GFP-specific and anti-myc-specific antibodies. Double staining indicated colocalization (yellow) of mutant ataxin-3 (green) and CA8 (red). Scale bar represents 50 μm. (b) HEK293 cells stably expressing GFP-tagged WT ataxin-3 (HEK293-GFP-MJD26), mutant ataxin-3 (HEK293-GFP-MJD78), and mutant ataxin-3 lacking N-terminal (HEK293-GFP-tMJD78) were analyzed by immunofluorescence using anti-GFP-specific and anti-CA8-specific antibodies. Double staining indicated colocalization (yellow) of ataxin-3 (green) and CA8 (red). Scale bar represents 50 μm

intracellular calcium release by an agonist of IP_3R1 (Chen et al., 2008). Additionally, CA8 was proved to interact with IP_3R1 and regulate Ca^{2+} release by influencing IP_3 binding to its receptor (IP_3R1) on the ER. Since we also observed the interesting interaction between mutant ataxin-3 and CA8, we next examined whether any alteration of Ca^{2+} release exists in SK-N-SH cells with and without mutant ataxin-3 and whether CA8 overexpression influences Ca^{2+} signaling. We first measured the calcium release in SK-N-SH cells with or without mutant ataxin-3, as well as in SK-MJD78 cells with or without CA8 overexpression under a 0.1 mM ATP stimulus. To block Ca^{2+} influx due to the activity of the store-operated channel, the experiment was performed in the absence of extracellular Ca^{2+} ions. Under our experimental conditions, the increase in cytosolic Ca^{2+} after the addition of ATP was largely from the ER pool. Our results demonstrated that ATP induced a transient elevation of Ca^{2+} for all tested cell lines. As shown in Figure 10a, cells harboring mutant ataxin-3 (SK-MJD78) showed a significantly increased cytosolic Ca^{2+} signaling in response to ATP compared with that in the WT cells (SK-N-SH cells) (p = 0.008). As expected, SK-MJD78-CA8 cells showed a reduced cytosolic Ca^{2+} signaling as compared with that in SK-MJD78-eGFP cells (Figure 10b) (p = 0.018).

Meanwhile, we also tried to determine whether overexpression of CA8 decreases cytosolic Ca^{2+} signaling in MJD CGNs. Our results demonstrated that even though no significant difference of

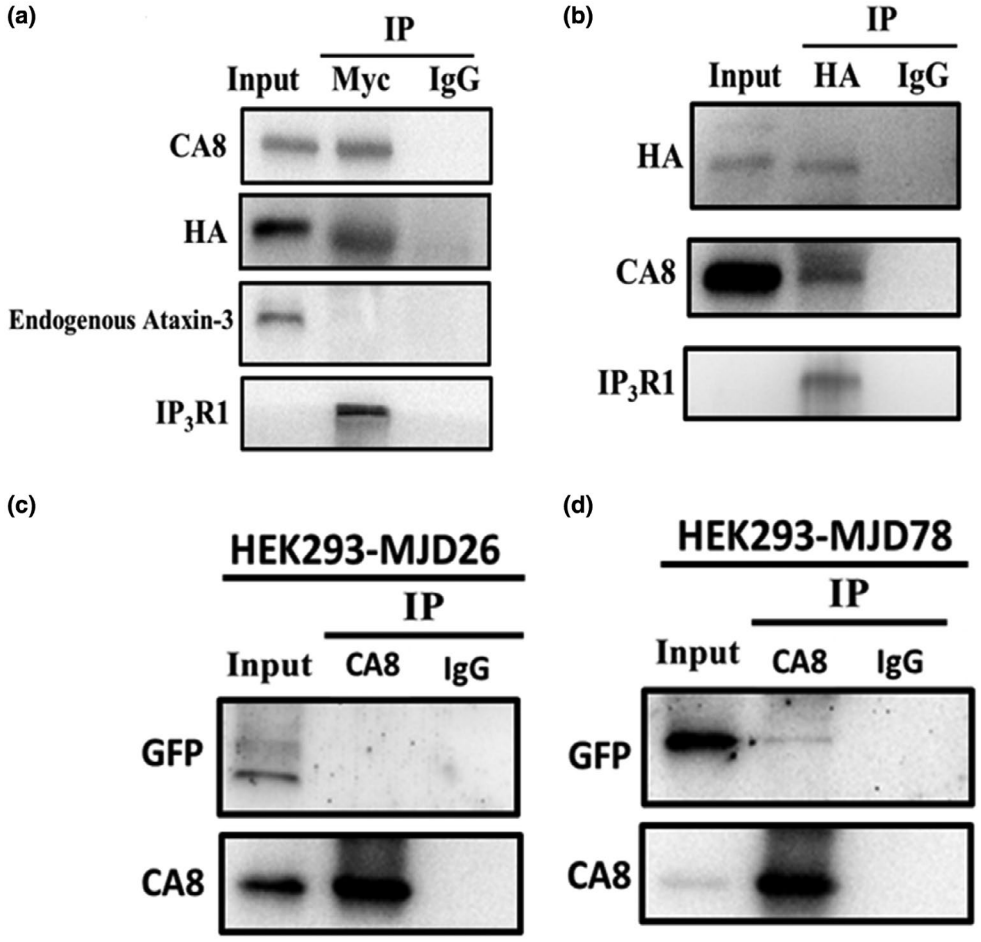

FIGURE 6 CA8 interacted with mutant ataxin-3 in SK-MJD78-CA8 and HEK293 cells stably expressing GFP-tagged mutant ataxin3 (HEK293-GFP-MJD78). (a) The cell lysates from SK-MJD78-CA8 were precipitated by anti-myc (CA8-tagged) and analyzed by Western blotting with anti-HA (MJD78-tagged). (b) The cell lysates from SK-MJD78-CA8 were precipitated by anti-HA and analyzed by Western blotting with anti-myc. The cell lysates from HEK293-MJD26 (c) and HEK293-MJD78 (d) were precipitated by anti-CA8 and analyzed by Western blotting with anti-GFP. The input lanes containing 1/50 of cell lysates was used for IP experiments. IgG was used as a negative control. Immunoblotting by the use of anti-IP_3R1 was used as control because IP_3R1 was known to interact with ataxin-3 and CA8

Ca^{2+} release was detected between WT CGNs infected with lentiviral CA8 and lentiviral eGFP (Figure 11b), both WT and MJD CGNs with downregulated CA8 showed significantly increased cytosolic Ca^{2+} signaling as compared with that of the lentiviral control infected CGNs (Figure 11a,c) ($p < 0.001$, Figure 11a; $p = 0.009$, Figure 11c). Consistently, overexpression of CA8 in MJD CGNs significantly decreased abnormal calcium release as compared with that of the lentiviral control infected CGNs (Figure 11d) ($p = 0.01$). Taken together, our findings confirm the abnormal Ca^{2+} release in neuronal cells harboring mutant ataxin-3 and further demonstrate that overexpression of CA8 rescues the abnormal Ca^{2+} signaling induced by mutant ataxin-3.

3.8 | Calcium ionophore counteracts the protective effect of CA8 in SK-MJD78-CA8 cells and in MJD CGNs

To examine the effects of CA8 on Ca^{2+}-induced cell survival, we next treated cells with different agents that are known to influence the Ca^{2+} influx. Calcium ionophore A23187, a mobile ion carrier that forms stable complexes with divalent cations (Pressman, 1976), is commonly used to increase intracellular calcium levels. So in order to correlate intracellular calcium concentration and cell survival, we examined the effects of A23187 on SK-MJD78 cells with and without CA8 overexpression under oxidative stress. As shown in Figure 12a, when SK-MJD78-CA8 cells were treated with calcium ionophore, a significant decrease in cell survival was observed ($p < 0.001$), as compared with cells without A23187 treatment, suggesting that calcium ionophore-induced calcium release counteracted the protective effect of CA8. Meanwhile, to determine whether the same effect would be observed in MJD CGNs, MJD CGNs were also subjected to calcium ionophore treatment. As shown in Figure 12b, after being pretreated with calcium ionophore, MJD CGNs with overexpressed CA8 had significantly decreased cell survival as compared with MJD CGNs treated with H_2O_2 only ($p = 0.007$). Moreover, it is noted that when MJD CGNs with overexpressed CA8 were treated with calcium ionophore, cell survival was reduced to the level similar to that in MJD CGNs without overexpressed CA8 treated with H_2O_2 alone (Figure 12b). Our results suggest that calcium ionophore treatment

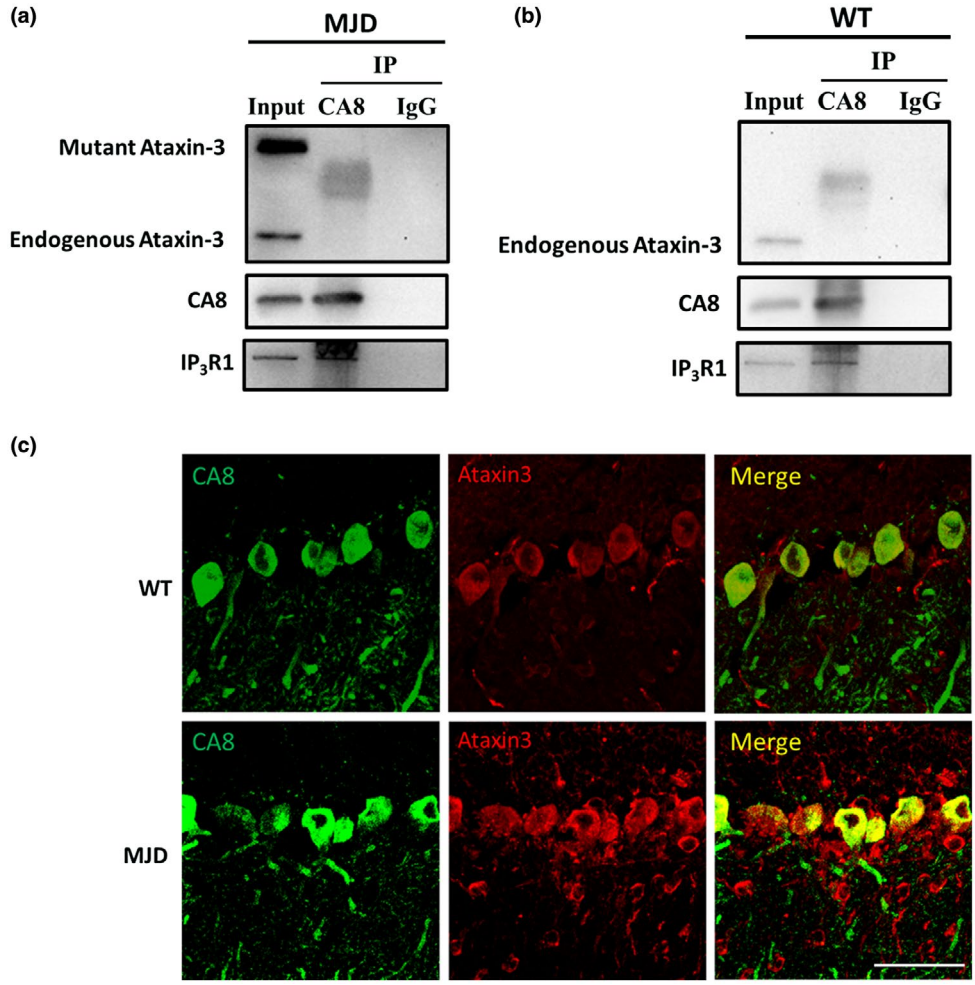

FIGURE 7 The interaction and localization between CA8 and mutant ataxin-3 in the MJD Tg mouse model. The cerebellum tissue lysates from MJD Tg mice of 52 weeks (a) and the age-matched WT control (b) were precipitated by anti-CA8 and analyzed by Western blotting with anti-ataxin-3 and anti-IP_3R1 (n = 3/group). The input lanes contain 1/50 of cell lysates used for IP experiments. IgG was used as a negative control. (c) CA8 was co-localized with mutant ataxin-3 in the MJD Tg mouse model. Expression and localization of CA8 and ataxin-3 were examined in the cerebellums of 52-week-old MJD Tg mice and the age-matched WT control by immunofluorescent staining. Double staining indicated colocalization (yellow) of CA8 (green) and ataxin-3 (red). Scale bar represents 50 μm. Independent experiments were repeated three times

in either SK-MJD78-CA8 or MJD CGNs with overexpressed CA8 counteracted the protective effect of CA8.

3.9 | BAPTA-AM shows no effect on cell survival in SK-MJD78-CA8 cells and MJD CGNs with overexpressed CA8

BAPTA-AM, (N,N′-[1,2-ethanediylbis (oxy-2,1-phenylene)] bis [N-[2-[(acetyloxy) methoxy]-2-oxoethyl]-1,1′-bis[(acetyloxy)methyl] ester-glycine), is membrane permeable calcium chelator that is commonly used to evaluate the role of intracellular calcium in cell signaling (Lee et al., 2012). Thus, we also examined whether BAPTA-AM pretreatment may alter cell survival in cells with or without overexpressed CA8 under H_2O_2 challenge. As shown in Figure 13a, cell survival in BAPTA-AM-pretreated SK-MJD-eGFP cells was significantly increased compared with that in cells without BAPTA-AM pretreatment (p = 0.004). However, BAPTA-AM pretreatment showed no effects on cell survival in SK-MJD78-CA8 cells upon H_2O_2 treatment (p = 0.862). Consistently, even though a significant increase in the cell survival was observed in MJD-eGFP CGNs with BAPTA-AM pretreatment (p < 0.001), cell survival showed no significant difference in CA8 overexpressing MJD CGNs with and without BAPTA-AM pretreatment (Figure 13b) (p = 0.741). Therefore, our results support the notion that BAPTA-AM has no obvious effect on cell survival in SK-MJD78-CA8 cells and MJD CGNs with overexpressed CA8.

3.10 | Calpeptin shows no significant effect on cell survival in MJD mutant cells with CA8 overexpression

Calpain is a cysteine proteases that is dependent on calcium to attain functionally active forms (Saez, Ramirez-Lorca, Moron, & Ruiz, 2006). It is known that altered calpain activity was associated

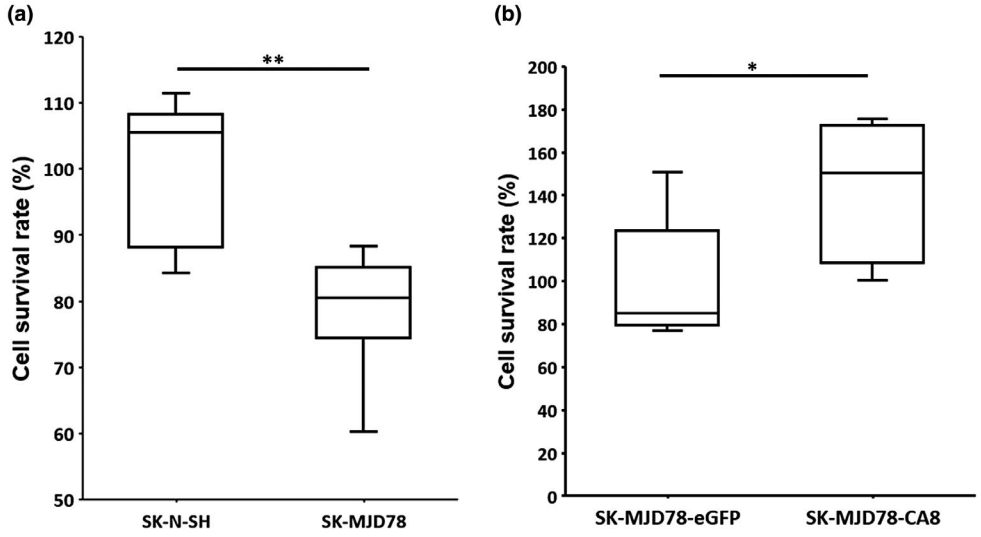

FIGURE 8 Overexpression of CA8 decreased cell death upon H_2O_2 treatment. (a) SK-N-SH cells showed increased cell survival than that in mutant SK-MJD78 cells. (b) SK-MJD78-CA8 cells were more resistant to oxidative stress as compared with that of SK-MJD78-eGFP cells. Data were presented from three independent experiments, each performed in triplicate. $^{*}p < 0.05$, $^{**}p < 0.01$. (Student's *t* test)

with the cleavage of mutant ataxin-3 in MJD disease (Haacke et al., 2007). Calpeptin, an inhibitor of calpains, is a cell permeable calpain inhibitor (Wang, 1990). Thus, we wanted to determine whether calpeptin pretreatment inhibits calpain activity and alters MJD cell survival when cells are challenged with H_2O_2. As shown in Figure 14, the survival rates of the SK-MJD78-eGFP cells and MJD-eGFP CGNs pretreated with calpeptin were moderately higher than that of the control cells treated with H_2O_2 only. However, the cell survival rate showed no difference in SK-MJD78-CA8 cells with and without calpeptin pretreatment (Figure 14a) ($p = 0.714$), nor any difference in MJD-CA8 CGNs (Figure 14b) ($p = 0.349$). Taken together, our results demonstrate that calpeptin has no further effect on cell survival in MJD mutant cells with CA8 overexpression.

4 | DISCUSSION

We have previously demonstrated that the expression level of CA8 is higher in human neuroblastoma cells harboring mutant ataxin-3 (Hsieh et al., 2013). In order to validate the expression levels of CA8 in a MJD animal model, we obtained MJD Tg mice (Cemal et al., 2002) and WT mice for comparison. We found that the mRNA and protein levels of CA8 were both moderately increased in MJD Tg mice (Figure 1). Considering CA8 was detected mainly in Purkinje cells (Bae et al., 2009), we further examined the expression pattern of CA8 by immunohistochemical staining. Our results confirmed that CA8 was expressed mainly in Purkinje cells, with more intense staining in MJD Tg mice as compared to that of the WT control (Figure 2). To assess the intensity in the immunohistochemical staining, we used a scoring system that takes into account the various staining intensity of the positive signals (Tsai et al., 2014). It is noted that CA8 expression was significantly increased in the cerebellum of MJD mice at the age of 3 weeks, 26 weeks, and 52 weeks; supporting the notion that mutant ataxin-3 expression contributes to the increase in CA8 expression. Interestingly, we observed a gradual decrease in CA8 expression with age in MJD Tg mice only. Considering the findings that CA8 overexpression desensitizes neuronal cells to staurosporine-induced apoptotic stress and loss-of-function of *ca8* gene results in abnormal movement pattern in zebrafish (Huang et al., 2014) and *waddles* mice (Jiao et al., 2005), we speculated that the decreased CA8 expression, observed in MJD Tg mice of 52 weeks as compared with that in MJD Tg mice of 3 weeks, may be relevant to the disease's late onset and progression.

To study the mechanism underlying the altered CA8 expression in the presence of mutant ataxin-3, we established three human embryonic kidney cell lines containing WT ataxin-3 (MJD26), mutant ataxin-3 (MJD78), and N-terminus truncated mutant ataxin-3 (tMJD78), respectively, for assaying the transcription activity of *hCA8* gene. Western blot was performed to assess the ectopic ataxin-3 expression in these stable clones. It was noted that the expression of truncated ataxin-3 was not detected by ataxin-3 antibody. Because ataxin-3 antibody was raised against region E214-L233 of the N-terminal Josephin domain, which was truncated from tMJD78, the expression of truncated ataxin-3 was confirmed by tagged GFP antibody (Figure 3b). Furthermore, transient transfection of luciferase reporter plasmid containing the full-length CA8 promoter was performed to determine the transcription activity of *hCA8* gene in the three stable clones. Consistent with our previous report (Hsieh et al., 2013), the results confirm that the CA8 expression is transcriptionally upregulated by the full length mutant ataxin-3. However, no detectable increase in CA8 transcript was observed in the presence of truncated ataxin-3. Even though we have yet to understand the detailed mechanism involved, transcriptional dysregulation has been implicated to play a central role in the SCA3

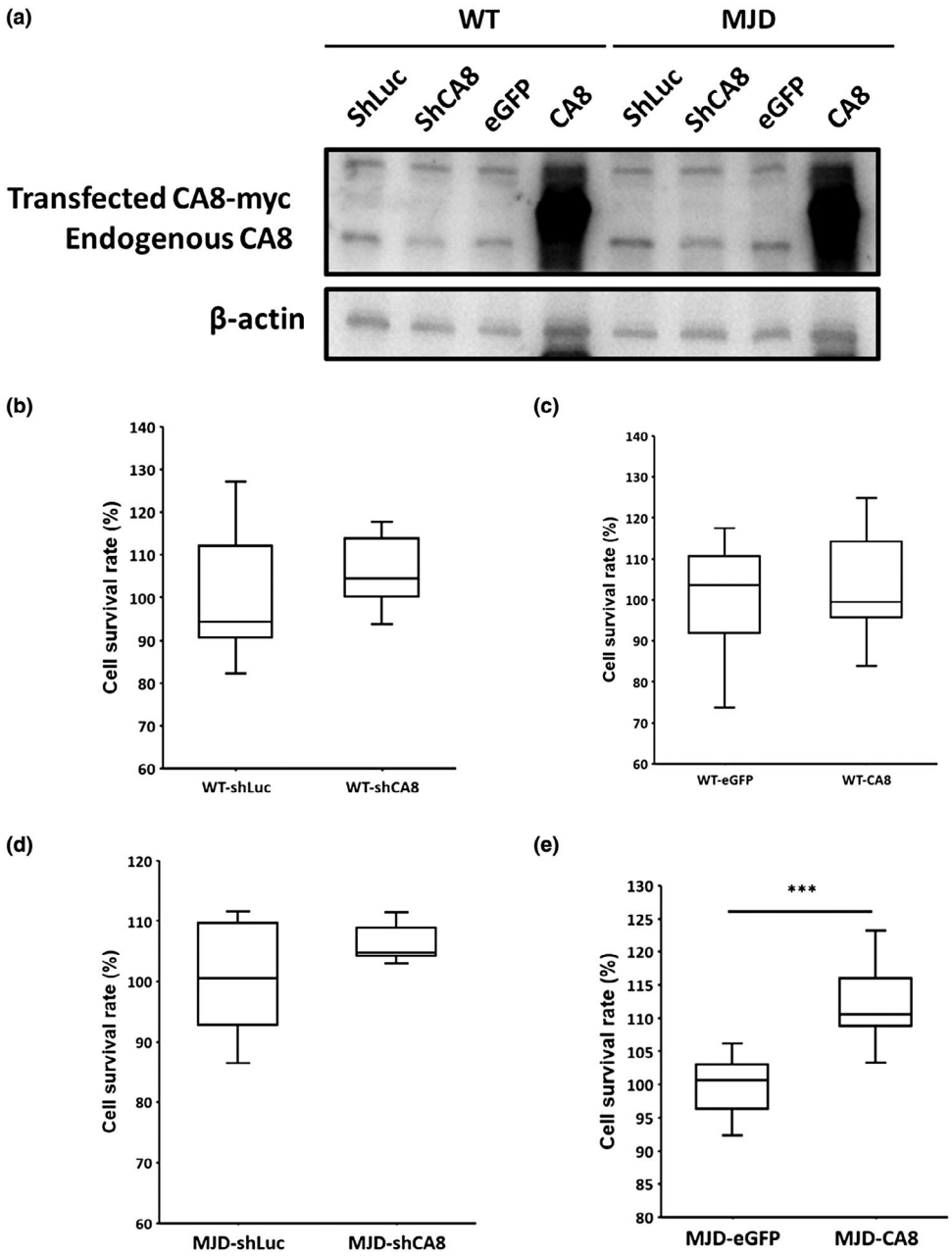

FIGURE 9 Overexpression of CA8 in MJD CGNs increased cell survival upon H_2O_2 treatment. (a) Western blot analysis of CA8 in CGNs with downregulated and overexpressed CA8. CGNs from WT and MJD Tg mice were infected with CA8 shRNA lentivirus (shCA8), CA8 overexpression lentivirus (CA8), and control virus (eGFP and shLuc) according to the standard protocol. (b and c) CGNs from WT mouse with or without CA8 expression showed no significant difference in cell survival under oxidative stress. (d) CGNs from MJD Tg mouse with downregulated CA8 showed no significant differences in cell survival under oxidative stress. (e) MJD CGNs with overexpressed CA8 were more resistant to oxidative stress as compared with MJD CGNs with eGFP control. Data were presented from at least three independent experiments, each performed in triplicate. ***$p < 0.001$. (Student's *t* test)

pathogenesis (Riley & Orr, 2006). It is likely that mutant ataxin-3, but not the truncated form, is involved in the transcriptional regulation of *hCA8* gene via chromatin binding or interaction with transcriptional regulators (Evert et al., 2006; Lo et al., 2018).

Our previous studies have shown that transient expression of mutant ataxin-3 altered the expression of CA11 in SK-N-SH cells and CA11 was redistributed into the nuclei, aggregated in cells expressing truncated ataxin-3 (Hsieh et al., 2013). For CA8, it was previously noted to be located in the cytoplasm (Aspatwar et al., 2010). Thus, whether CA8 is redistributed into the nuclei in the presence of mutant ataxin-3 remains to be addressed. As such, immunofluorescence was carried out to examine the cellular localization of CA8 and mutant ataxin-3. Our results showed that CA8 was mainly distributed in the cytoplasm and co-localized, at least partially, with WT, mutant or truncated ataxin-3 (Figure 5); suggesting that the cellular localization of CA8 was not altered

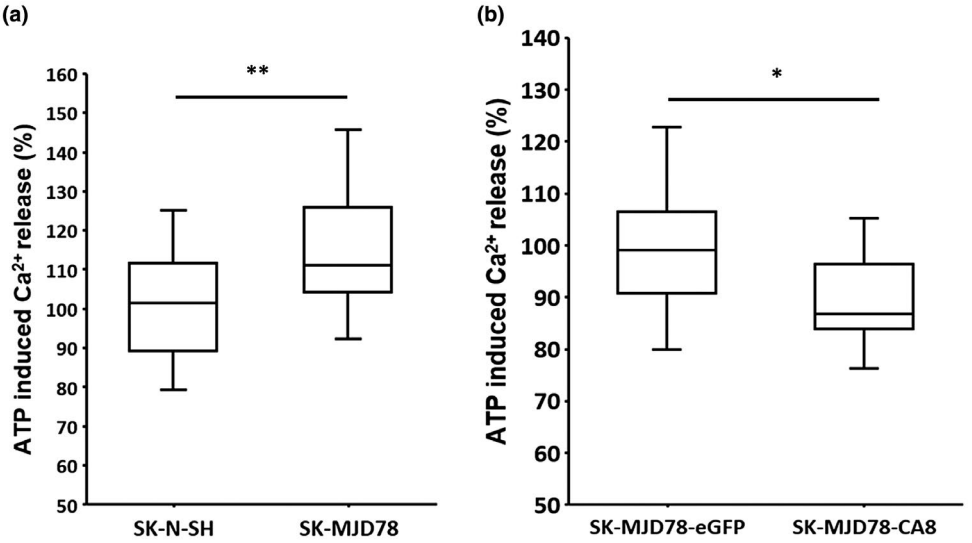

FIGURE 10 CA8 rescued abnormal Ca^{2+} release in SK-MJD78-CA8 cells. Cytosolic calcium signals in response to 0.1 mM ATP. Fura-4M fluorescence was recorded continuously at 37°C in a spectrofluorometer at excitation wavelength of 494 nm and an emission wavelength of 516 nm. (a) Increased Ca^{2+} release was observed in SK-MJD78 cells as compared with that in SK-N-SH cells. (b) Overexpression of CA8 in SK-MJD78-CA8 cells decreased the abnormal Ca^{2+} release. Data were presented from three independent experiments, each performed in triplicate. $^{*}p < 0.05$, $^{**}p < 0.01$. (Student's *t* test)

by mutant ataxin-3. In addition, immunoprecipitation revealed that CA8 interacted with mutant ataxin-3 in SK-MJD78-CA8 and HEK293-MJD78 cells (Figure 6). It is worth noting that the interaction between mutant ataxin-3 and the novel protein CA8 in MJD disease cellular model was first reported in this study. Even though we were not able to confirm the interaction between the endogenous CA8 and mutant ataxin-3 using cerebellar tissue lysates from Tg MJD and WT mice (Figure 7a,b), our results from immunofluorescence further demonstrated that mutant ataxin-3 and CA8 were co-localized, at least partially, in the Purkinje layer of mouse cerebellum (Figure 7c). This discrepancy between the immunoprecipitation data obtained from cellular and animal models may be due to a relatively weak interaction between CA8 and mutant ataxin-3. In other words, we suspect that the amount of endogenous CA8 is not enough to precipitate the weakly interacting mutant ataxin-3 in our experimental settings. However, more investigations are warranted to clarify the physical interaction between CA8 and mutant ataxin-3 in vivo.

We have previously shown that the neuroblastoma cells containing mutant ataxin-3, SK-MJD78, are more susceptible to oxidative stress than the control cells (Wen et al., 2003). Moreover, we found a protective function of CA8 in cells harboring the A8344G mutation of mitochondrial DNA (Wang et al., 2014). Additionally, CA8 knockdown was reported to impair brain development through increased neuronal cell death (Aspatwar et al., 2013). Thus, we speculated that the significantly increased expression of CA8 in MJD Tg mice may play an important protective role in the early disease stage and may be relevant to the late onset of the disease. To investigate the possible protective role of CA8, ROS stress was applied and cell survival was assessed in both SK-N-SH MJD cellular model and in primary CGNs with different expression levels of CA8. As expected, overexpression of CA8 significantly increased the cell survival rate of SK-MJD78-CA8 cells as compared with that of the SK-MJD78-eGFP cells after H_2O_2 treatment (Figure 8b). Moreover, MJD CGNs with overexpressed CA8 significantly increased the cell survival as compared with that of the lentiviral control infected CGNs after H_2O_2 treatment (Figure 9e). Our results support a general protective role of CA8 in both MJD neuronal cells and in MJD CGNs. However, under H_2O_2 treatment, the cell survival rate of WT or MJD CGNs with downregulated CA8 failed to show any significant alteration as compared with that of WT or MJD CGNs infected with the lentiviral control (Figure 9b,d). It was noted the downregulation of CA8 by lentiviral shCA8 only reduced the CA8 expression levels to 50 and 43% of that in the WT and MJD CGNs (Figure 9a), respectively, which may explain why CGNs with downregulated CA8 did not show significant alteration in cell survival.

As reported previously, mutant ataxin-3 interacts with IP_3R1 and activates the intracellular calcium release by an agonist of IP_3R1 (Chen et al., 2008), suggesting that abnormal neuronal Ca^{2+} signaling plays an important role in the pathogenesis of SCA3 (Bezprozvanny, 2009; Chen et al., 2008). On the other hand, it is known that CA8 interacts with IP_3R1 and suppresses the binding affinity of IP_3 to the receptor IP_3R1 (Hirota et al., 2003), resulting in a decrease in calcium release. Given that the disease progression may be related to the opposing effects of CA8 and mutant ataxin-3 on controlling calcium release, we carefully examined the effects of CA8 on Ca^{2+} signaling in the presence of mutant ataxin-3 in the MJD cellular and animal models. As expected, a significant decrease in calcium release was observed in SK-MJD78-CA8 cells, as compared with SK-MJD78-eGFP cells (Figure 10b). Similarly, our results showed a significant decrease in calcium release in MJD CGNs with overexpression of CA8 as compared with the lentiviral control infected neurons

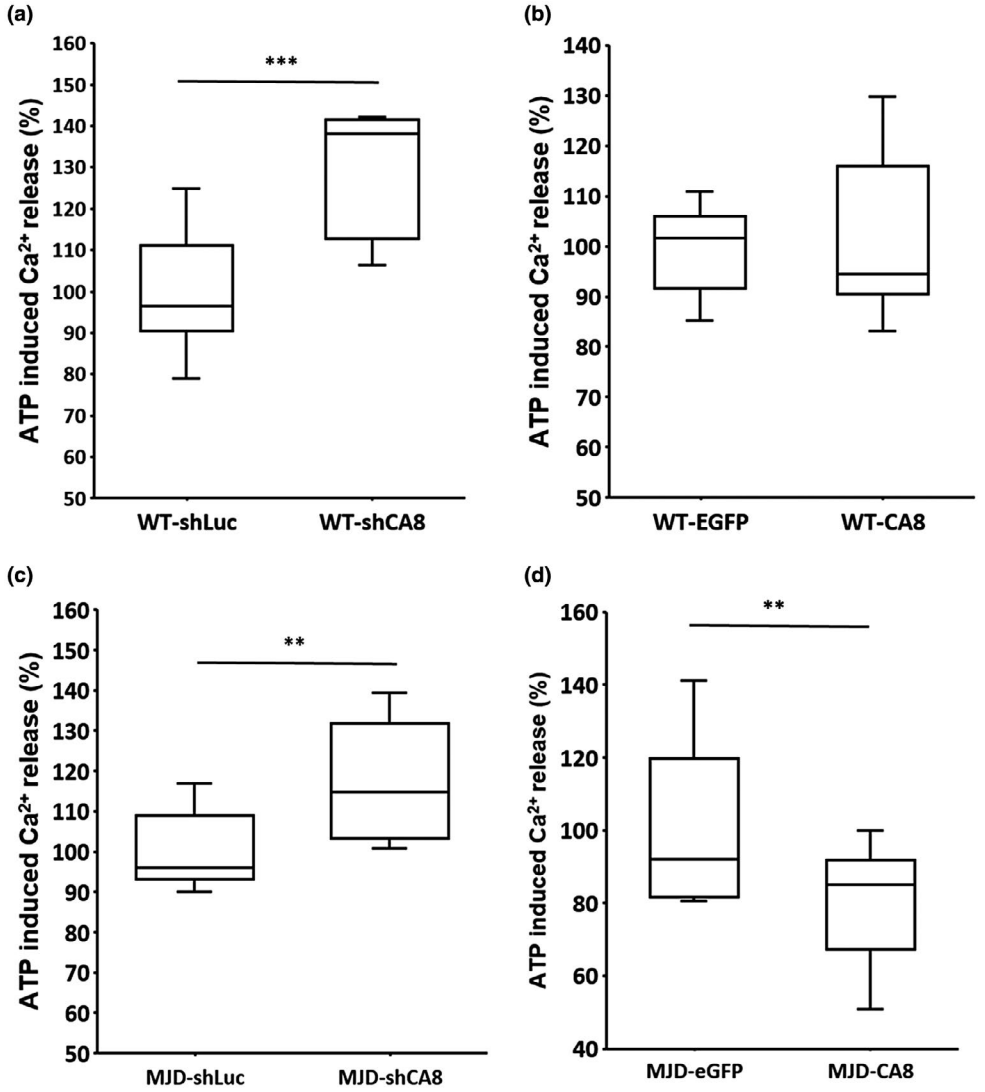

FIGURE 11 Decreased ER-dependent Ca^{2+} release in MJD CGNs with CA8 overexpression. CGNs from WT and MJD Tg mice were infected with CA8 shRNA lentivirus (shCA8), CA8 overexpression lentivirus (CA8), and control virus (eGFP and shLuc). Increased Ca^{2+} release was observed in both WT-shCA8 (a) and MJD-shCA8 (c) as compared with that of the control (shLuc). Overexpressed CA8 in WT CGNs showed no difference in calcium release as compared with that in WT-eGFP CGNs (b). Overexpressed CA8 in MJD CGNs rescued the abnormal Ca^{2+} release in MJD-eGFP (d). Data were presented from three independent experiments, each performed at least in triplicate. $^{**}p < 0.01$, $^{***}p < 0.001$. (Student's *t* test)

(Figure 11d). These findings demonstrate that the increased expression of CA8 rescues the abnormal calcium release induced by mutant ataxin-3, which may be important for the increased cell survival rate in SK-MJD-CA8 (Figure 8b) and MJD CGNs with overexpressed CA8 (Figure 9e). In contrast, there was no difference of calcium release between WT CGNs with overexpressed CA8 and the lentiviral control (Figure 11b), indicating that overexpression of CA8 had no further effect on the calcium release in WT CGNs with endogenous CA8 expression. Interestingly, both WT and MJD CGNs with downregulated CA8 showed a significant increase in Ca^{2+} signaling compared with those in control WT and MJD CGNs (Figure 11a,c), even though the reduction of CA8 was only less than 50% in the shRNA treated CGNs. However, the increased Ca^{2+} release accompanied by downregulated CA8 did not directly correlate to an increase in cell death (Figure 9), suggesting that the increased Ca^{2+} release was only a contributing factor in triggering cell death. Taken together, our observation support the notion that overexpression of CA8 is critical in the modulation of intracellular Ca^{2+} signaling, which may be responsible for the protective function in MJD neuroblastoma cells and in MJD CGNs.

In order to further clarify the effects of CA8 on Ca^{2+} release in cells with or without mutant ataxin-3, we used various drugs to manipulate the calcium release in neuroblastoma cells and in CGNs. For instance, calcium ionophore A23187 was used to increase intracellular Ca^{2+} levels. It is noted that the cell survival rate of SK-N-SH and WT CGNs under H_2O_2 treatment was not affected by the addition of calcium ionophore (data not shown). Under the calcium ionophore treatment, cell survival in SK-MJD78-CA8 or MJD CGNs with

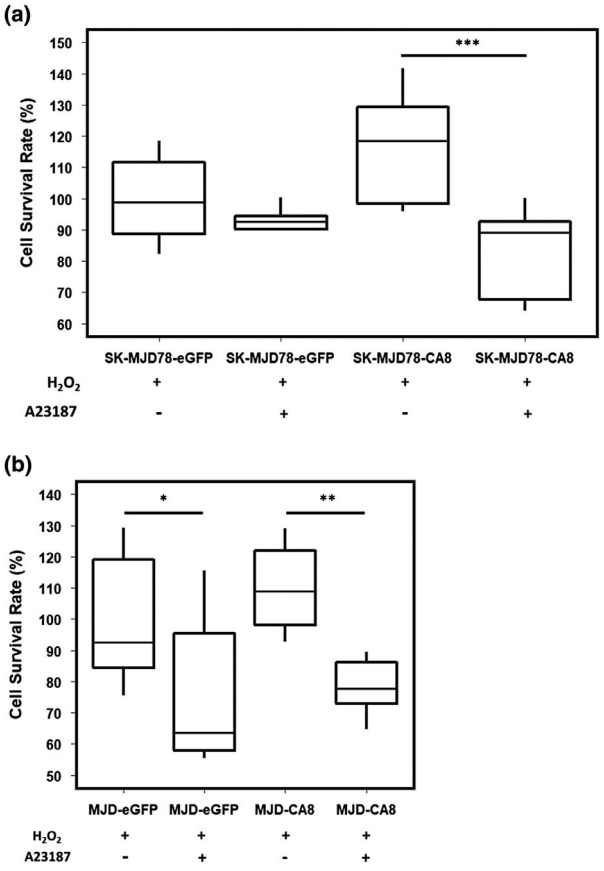

FIGURE 12 Ca^{2+} ionophore treatment (A23187) in SK-MJD78 cells and MJD CGNs with or without overexpressed CA8. SK-MJD78 cells and MJD CGNs were treated with A23187 to increase Ca^{2+} release and then cells were challenged with H_2O_2. Cell viability was determined with MTT assay. (a) Ca^{2+} ionophore decreased cell survival in SK-MJD78-CA8 cells. (b) Ca^{2+} ionophore decreased cell survival in MJD-eGFP and MJD-CA8 cells under oxidative stress. Data were presented from three independent experiments, each performed in triplicate. $^{*}p < 0.05$, $^{**}p < 0.01$, $^{***}p < 0.001$. (Two-way ANOVA followed by Tukey's HSD test)

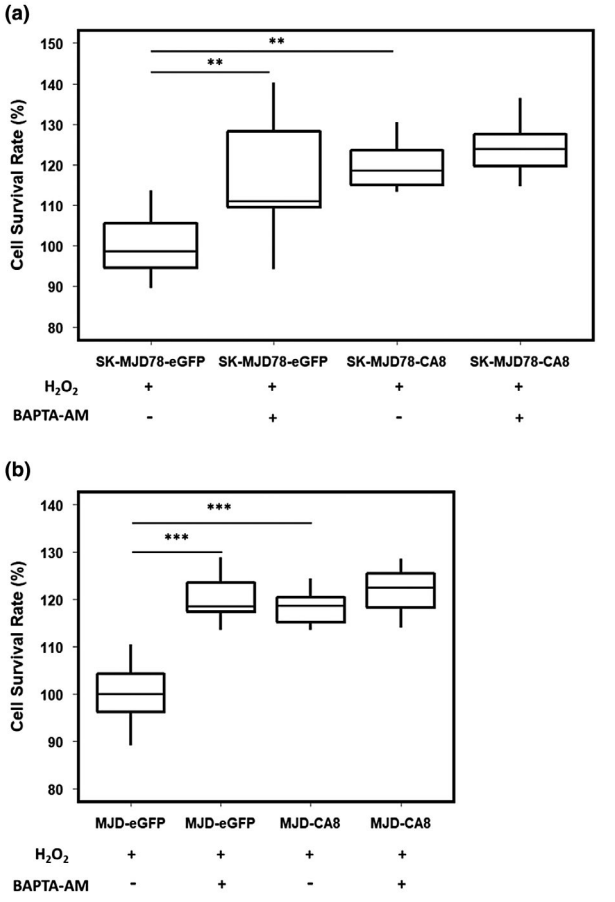

FIGURE 13 BAPTA-AM treatment in SK-MJD78 cells and MJD CGNs with different expression levels of CA8. SK-MJD78 cells and MJD CGNs were treated with BAPTA-AM and then cells were challenged with H_2O_2. Cell viability was determined with MTT assay. (a) BAPTA-AM increased cell survival in SK-MJD-eGFP cells but showed no effects on cell survival in SK-MJD78-CA8 cells. (b) BAPTA-AM increased cell survival in MJD-eGFP cells but showed no effects on cell survival in MJD CGNs with overexpressed CA8 cells. Data were presented from three independent experiments, each performed in triplicate. $^{**}p < 0.01$, $^{***}p < 0.001$. (Two-way ANOVA followed by Tukey's HSD test)

overexpressed CA8 showed a significant decrease, as compared with that of cells without calcium ionophore treatment; suggesting that the calcium ionophore-induced Ca^{2+} release might counteract the protective function of CA8 in cells harboring mutant ataxin-3. However, it is noted that no significant difference of cell survival was observed between cells with and without overexpressed CA8 under calcium ionophore treatment, which may be because the decreased calcium release accompanied by overexpressed CA8 is completely counteracted by the much greater calcium release induced by calcium ionophore. Additionally, BAPTA-AM is a well-known membrane permeable Ca^{2+} chelator and can be used to control the level of intracellular Ca^{2+} (Lee et al., 2012). Hence, we also tried to determine whether BAPTA-AM pre-treatment may decrease Ca^{2+} and alter cell survival in the MJD disease models. As shown in Figure 13, the cell survival in SK-MJD78-eGFP cells and MJD-eGFP CGNs increased after BAPTA-AM treatment (Figure 13a,b). However, SK-MJD78-CA8 cells and MJD CGNs with overexpressed CA8 did not show further increase in cell survival after BAPTA-AM treatment as compared with their controls, suggesting that calcium chelator fails to further reduce calcium release in cells harboring overexpressed CA8. Taken together, our results support and extend the notion that CA8 has an important function to rescue abnormal Ca^{2+} release and decrease cell death in a MJD neuroblastoma cellular model and in primary CGNs from MJD Tg mice.

On the other hand, the calcium-induced activation of calpain has been shown to be responsible for mutant ataxin-3 cleavage in MJD disease (Haacke et al., 2007). It is known that calpeptin, a calpain inhibitor, treatment resulted in reduced mutant ataxin-3 proteolysis and prevented cell toxicity in neurodegenerative disease models (Haacke et al., 2006, 2007; Simoes et al., 2012). Therefore, we also treated MJD neuroblastoma cells and CGNs with calpeptin and assayed for the cell survival under H_2O_2 challenge. As expected,

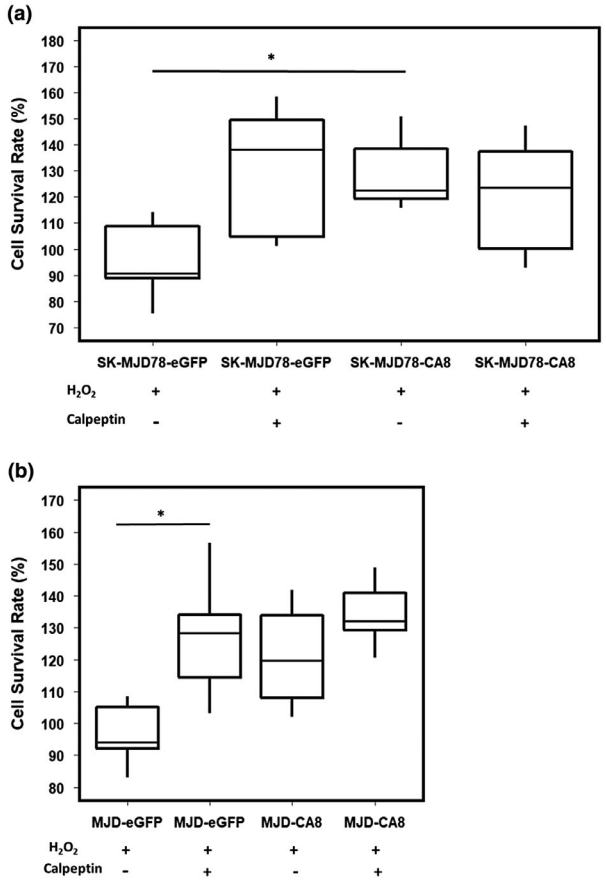

FIGURE 14 Calpeptin treatment in SK-MJD78 cells and MJD CGNs with or without overexpressed CA8. SK-MJD78 cells and MJD CGNs were treated with calpeptin and then cells were challenged with H_2O_2. Cell viability was determined with MTT assay. (a) Calpeptin showed no effects on cell survival in SK-MJD78-CA8 cells. (b) Calpeptin increased cell survival in MJD-eGFP cells but showed no effects on cell survival in MJD CGNs with overexpressed CA8 cells. Data were presented from three independent experiments, each performed in triplicate. $^*p < 0.05$. (Two-way ANOVA followed by Tukey's HSD test)

SK-MJD78-eGFP cells and MJD-eGFP CGNs pre-treated with calpeptin showed an increase in cell survival upon H_2O_2 challenge (Figure 14a,b), indicating that the calpeptin inhibited the function of calpain. However, SK-MJD78-CA8 cells and MJD CGNs with overexpressed CA8 did not show a significant alteration of cell survival after calpeptin treatment. Considering overexpression of CA8 in SK-MJD78 cells and in MJD CGNs rescued the abnormal Ca^{2+} release (Figures 10b, 11d), we speculated that the reduced calcium release due to overexpression of CA8 may have already led to inactivation of calpains. Therefore, SK-MJD78-CA8 cells and MJD CGNs with overexpression of CA8 treated with calpeptin did not show further increase in cell survival as compared with those without the calpeptin treatment.

In summary, our results revealed several important findings in Machado–Joseph disease. We demonstrate a significant increased expression of CA8 in MJD cerebellar tissues. The immunostaining of CA8 in MJD Tg mice was found to be dynamic and gradually decreasing with age. In addition, overexpression of CA8 desensitizes SK-MJD78 cells and MJD CGNs to H_2O_2 treatment, supporting the protective role of CA8 in MJD. Moreover, overexpression of CA8 in SK-MJD78-CA8 cells and in MJD CGNs results in a significant decrease in calcium release, indicating that the protective function may be via reduced calcium signaling. In the present study, we were the first to report the noval expression patterns of CA8 associated with the disease progression of MJD. We speculate that the declining expression of CA8 following an initial increased expression, a process that parallels the progression of the disease from early to late stages, may be related to the late onset phenomenon of the Machado–Joseph disease. It is possible that the initial significant increase in CA8 may carry out a protective function in the early stage of disease, followed by a decline in CA8 expression as the disease progresses. Even though an upregulated level of CA8 expression is still seen as compared to WT controls; CA8 cannot reverse the global dysfunction during the disease progress due to accumulation of cytotoxic effects. Although the detailed underlying mechanisms still need further investigations, we hope that our findings may provide important information for potential therapeutic targets in the future.

DECLARATION OF TRANSPARENCY

The authors, reviewers, and editors affirm that in accordance to the policies set by the Journal of Neuroscience Research, this manuscript presents an accurate and transparent account of the study being reported and that all critical details describing the methods and results are present.

ACKNOWLEDGMENTS

We thank the National RNAi Core Facility for providing the RNAi reagents; Drs. Shin-Lan Hsu and Hsi-Chi Lu for providing the cell lines; Dr. Henry Paulson for providing plasmids; Tang-Hao Chi for plasmid construction.

CONFLICT OF INTEREST

The authors declare no conflict of interest.

AUTHOR CONTRIBUTIONS

Conceptualization, M.H. and Y.T.L.; *Methodology*, B.Y.H., C.M.L., and Y.T.L.; *Validation*, M.H., B.Y.H., and C.Y.M.; *Formal Analysis*, M.H., B.Y.H., and C.Y.M.; *Investigation*, B.Y.H., C.Y.M., and Y.T.L.; *Resources*, M.H. and C.S.L.; *Writing—Original Draft*, M.H., B.Y.H., and Y.T.L.; *Writing—Review and Editing*, M.H. and B.Y.H.; *Visualization*, M.H., B.Y.H., C.Y.M., and Y.T.L.; *Supervision*, M.H.; *Funding Acquisition*, M.H.

DATA ACCESSIBILITY

The data that support the findings of this study are available from the corresponding author upon reasonable request.

ORCID

Mingli Hsieh https://orcid.org/0000-0002-8097-0466

REFERENCES

Aspatwar, A., Tolvanen, M. E. E., Jokitalo, E., Parikka, M., Ortutay, C., Harjula, S.-K., … Parkkila, S. (2013). Abnormal cerebellar development and ataxia in CARP VIII morphant zebrafish. *Human Molecular Genetics*, *22*(3), 417–432. https://doi.org/10.1093/hmg/dds438

Aspatwar, A., Tolvanen, M. E., & Parkkila, S. (2010). Phylogeny and expression of carbonic anhydrase-related proteins. *BMC Molecular Biology*, *11*, 25. https://doi.org/10.1186/1471-2199-11-25

Bae, Y.-K., Kani, S., Shimizu, T., Tanabe, K., Nojima, H., Kimura, Y., … Hibi, M. (2009). Anatomy of zebrafish cerebellum and screen for mutations affecting its development. *Developmental Biology*, *330*(2), 406–426. https://doi.org/10.1016/j.ydbio.2009.04.013

Berke, S. J., Schmied, F. A., Brunt, E. R., Ellerby, L. M., & Paulson, H. L. (2004). Caspase-mediated proteolysis of the polyglutamine disease protein ataxin-3. *Journal of Neurochemistry*, *89*(4), 908–918. https://doi.org/10.1111/j.1471-4159.2004.02369.x

Berthelsen, P. (1982). Cardiovascular performance and oxyhemoglobin dissociation after acetazolamide in metabolic alkalosis. *Intensive Care Medicine*, *8*(6), 269–274. https://doi.org/10.1007/BF01716736

Bezprozvanny, I. (2009). Calcium signaling and neurodegenerative diseases. *Trends in Molecular Medicine*, *15*(3), 89–100. https://doi.org/10.1016/j.molmed.2009.01.001

Burnett, B. G., & Pittman, R. N. (2005). The polyglutamine neurodegenerative protein ataxin 3 regulates aggresome formation. *Proceedings of the National Academy of Sciences of the United States of America*, *102*(12), 4330–4335. https://doi.org/10.1073/pnas.0407252102

Cemal, C. K., Carroll, C. J., Lawrence, L., Lowrie, M. B., Ruddle, P., Al-Mahdawi, S., … Chamberlain, S. (2002). YAC transgenic mice carrying pathological alleles of the MJD1 locus exhibit a mild and slowly progressive cerebellar deficit. *Human Molecular Genetics*, *11*(9), 1075–1094. https://doi.org/10.1093/hmg/11.9.1075

Chai, Y., Shao, J., Miller, V. M., Williams, A., & Paulson, H. L. (2002). Live-cell imaging reveals divergent intracellular dynamics of polyglutamine disease proteins and supports a sequestration model of pathogenesis. *Proceedings of the National Academy of Sciences of the United States of America*, *99*(14), 9310–9315. https://doi.org/10.1073/pnas.152101299

Chang, W. H., Tien, C. L., Chen, T. J., Nukina, N., & Hsieh, M. (2009). Decreased protein synthesis of Hsp27 associated with cellular toxicity in a cell model of Machado–Joseph disease. *Neuroscience Letters*, *454*(2), 152–156. https://doi.org/10.1016/j.neulet.2009.03.004

Chen, X., Tang, T.-S., Tu, H., Nelson, O., Pook, M., Hammer, R., … Bezprozvanny, I. (2008). Deranged calcium signaling and neurodegeneration in spinocerebellar ataxia type 3. *Journal of Neuroscience*, *28*(48), 12713–12724. https://doi.org/10.1523/JNEUROSCI.3909-08.2008

Coutinho, P., & Andrade, C. (1978). Autosomal dominant system degeneration in Portuguese families of the Azores Islands. A new genetic disorder involving cerebellar, pyramidal, extrapyramidal and spinal cord motor functions. *Neurology*, *28*(7), 703–709.

Durcan, T. M., & Fon, E. A. (2013). Ataxin-3 and its e3 partners: Implications for Machado–Joseph disease. *Frontiers in Neurology*, *4*, 46. https://doi.org/10.3389/fneur.2013.00046

Evert, B. O., Araujo, J., Vieira-Saecker, A. M., de Vos, R. A., Harendza, S., Klockgether, T., & Wullner, U. (2006). Ataxin-3 represses transcription via chromatin binding, interaction with histone deacetylase 3, and histone deacetylation. *Journal of Neuroscience*, *26*(44), 11474–11486. https://doi.org/10.1523/JNEUROSCI.2053-06.2006

Haacke, A., Broadley, S. A., Boteva, R., Tzvetkov, N., Hartl, F. U., & Breuer, P. (2006). Proteolytic cleavage of polyglutamine-expanded ataxin-3 is critical for aggregation and sequestration of non-expanded ataxin-3. *Human Molecular Genetics*, *15*(4), 555–568. https://doi.org/10.1093/hmg/ddi472

Haacke, A., Hartl, F. U., & Breuer, P. (2007). Calpain inhibition is sufficient to suppress aggregation of polyglutamine-expanded ataxin-3. *Journal of Biological Chemistry*, *282*(26), 18851–18856. https://doi.org/10.1074/jbc.M611914200

Hirota, J., Ando, H., Hamada, K., & Mikoshiba, K. (2003). Carbonic anhydrase-related protein is a novel binding protein for inositol 1,4,5-trisphosphate receptor type 1. *The Biochemical Journal*, *372*(Pt 2), 435–441. https://doi.org/10.1042/BJ20030110

Hsieh, M., Chang, W. H., Hsu, C. F., Nishimori, I., Kuo, C. L., & Minakuchi, T. (2013). Altered expression of carbonic anhydrase-related protein XI in neuronal cells expressing mutant ataxin-3. *Cerebellum*, *12*(3), 338–349. https://doi.org/10.1007/s12311-012-0430-2

Huang, M. S., Wang, T. K., Liu, Y. W., Li, Y. T., Chi, T. H., Chou, C. W., & Hsieh, M. (2014). Roles of carbonic anhydrase 8 in neuronal cells and zebrafish. *Biochimica Et Biophysica Acta*, *1840*(9), 2829–2842. https://doi.org/10.1016/j.bbagen.2014.04.017

Hubener, J., Weber, J. J., Richter, C., Honold, L., Weiss, A., Murad, F., … Nguyen, H. P. (2013). Calpain-mediated ataxin-3 cleavage in the molecular pathogenesis of spinocerebellar ataxia type 3 (SCA3). *Human Molecular Genetics*, *22*(3), 508–518. https://doi.org/10.1093/hmg/dds449

Jiao, Y., Yan, J., Zhao, Y. U., Donahue, L. R., Beamer, W. G., Li, X., … Gu, W. (2005). Carbonic anhydrase-related protein VIII deficiency is associated with a distinctive lifelong gait disorder in waddles mice. *Genetics*, *171*(3), 1239–1246. https://doi.org/10.1534/genetics.105.044487

Kawaguchi, Y., Okamoto, T., Taniwaki, M., Aizawa, M., Inoue, M., Katayama, S., … Kakizuka, A. (1994). CAG expansions in a novel gene for Machado–Joseph disease at chromosome 14q32.1. *Nature Genetics*, *8*(3), 221–228. https://doi.org/10.1038/ng1194-221

Kaya, N., Aldhalaan, H., Al-Younes, B., Colak, D., Shuaib, T., Al-Mohaileb, F., … Al-Owain, M. (2011). Phenotypical spectrum of cerebellar ataxia associated with a novel mutation in the CA8 gene, encoding carbonic anhydrase (CA) VIII. *American Journal of Medical Genetics. Part B, Neuropsychiatric Genetics: The Official Publication of the International Society of Psychiatric Genetics*, *156B*(7), 826–834. https://doi.org/10.1002/ajmg.b.31227

Laco, M. N., Oliveira, C. R., Paulson, H. L., & Rego, A. C. (2012). Compromised mitochondrial complex II in models of Machado–Joseph disease. *Biochimica Et Biophysica Acta*, *1822*(2), 139–149. https://doi.org/10.1016/j.bbadis.2011.10.010

Lee, G.-S., Subramanian, N., Kim, A. I., Aksentijevich, I., Goldbach-Mansky, R., Sacks, D. B., … Chae, J. J. (2012). The calcium-sensing receptor regulates the NLRP3 inflammasome through Ca2+ and cAMP. *Nature*, *492*(7427), 123–127. https://doi.org/10.1038/nature11588

Lo, C. M., Ma, Y. S., Wei, Y. H., Hsieh, B. Y. T., & Hsieh, M. (2018). Promoter analysis and transcriptional regulation of human carbonic anhydrase VIII gene in a MERRF disease cell model. *Archives of Biochemistry and Biophysics*, *641*, 50–61. https://doi.org/10.1016/j.abb.2018.01.012

McCampbell, A., Taylor, J. P., Taye, A. A., Robitschek, J., Li, M., Walcott, J., … Fischbeck, K. H. (2000). CREB-binding protein sequestration by expanded polyglutamine. *Human Molecular Genetics*, *9*(14), 2197–2202. https://doi.org/10.1093/hmg/9.14.2197

Mueller, T., Breuer, P., Schmitt, I., Walter, J., Evert, B. O., & Wullner, U. (2009). CK2-dependent phosphorylation determines cellular localization and stability of ataxin-3. *Human Molecular Genetics*, *18*(17), 3334–3343. https://doi.org/10.1093/hmg/ddp274

Picaud, S. S., Muniz, J. R., Kramm, A., Pilka, E. S., Kochan, G., Oppermann, U., & Yue, W. W. (2009). Crystal structure of human carbonic anhydrase-related protein VIII reveals the basis for catalytic silencing. *Proteins*, *76*(2), 507–511. https://doi.org/10.1002/prot.22411

Pressman, B. C. (1976). Biological applications of ionophores. *Annual Review of Biochemistry*, *45*, 501–530. https://doi.org/10.1146/annurev.bi.45.070176.002441

Riess, O., Rub, U., Pastore, A., Bauer, P., & Schols, L. (2008). SCA3: Neurological features, pathogenesis and animal models. *Cerebellum*, *7*(2), 125–137. https://doi.org/10.1007/s12311-008-0013-4

Riley, B. E., & Orr, H. T. (2006). Polyglutamine neurodegenerative diseases and regulation of transcription: Assembling the puzzle. *Genes & Development*, *20*(16), 2183–2192. https://doi.org/10.1101/gad.1436506

Rosenberg, R. N. (1992). Machado–Joseph disease: An autosomal dominant motor system degeneration. *Movement Disorders*, *7*(3), 193–203. https://doi.org/10.1002/mds.870070302

Saez, M. E., Ramirez-Lorca, R., Moron, F. J., & Ruiz, A. (2006). The therapeutic potential of the calpain family: New aspects. *Drug Discovery Today*, *11*(19–20), 917–923. https://doi.org/10.1016/j.drudis.2006.08.009

Shimohata, T., Nakajima, T., Yamada, M., Uchida, C., Onodera, O., Naruse, S., … Tsuji, S. (2000). Expanded polyglutamine stretches interact with TAFII130, interfering with CREB-dependent transcription. *Nature Genetics*, *26*(1), 29–36. https://doi.org/10.1038/79139

Simoes, A. T., Goncalves, N., Koeppen, A., Deglon, N., Kugler, S., Duarte, C. B., & Pereira de Almeida, L. (2012). Calpastatin-mediated inhibition of calpains in the mouse brain prevents mutant ataxin 3 proteolysis, nuclear localization and aggregation, relieving Machado–Joseph disease. *Brain*, *135*(Pt 8), 2428–2439. https://doi.org/10.1093/brain/aws177

Simões, A. T., Gonçalves, N., Nobre, R. J., Duarte, C. B., & Pereira de Almeida, L. (2014). Calpain inhibition reduces ataxin-3 cleavage alleviating neuropathology and motor impairments in mouse models of Machado–Joseph disease. *Human Molecular Genetics*, *23*(18), 4932–4944. https://doi.org/10.1093/hmg/ddu209

Sjoblom, B., Elleby, B., Wallgren, K., Jonsson, B. H., & Lindskog, S. (1996). Two point mutations convert a catalytically inactive carbonic anhydrase-related protein (CARP) to an active enzyme. *FEBS Letters*, *398*(2–3), 322–325. https://doi.org/10.1016/S0014-5793(96)01263-X

Soong, B., Cheng, C., Liu, R., & Shan, D. (1997). Machado–Joseph disease: Clinical, molecular, and metabolic characterization in Chinese kindreds. *Annals of Neurology*, *41*(4), 446–452. https://doi.org/10.1002/ana.410410407

Takahashi, T., Kikuchi, S., Katada, S., Nagai, Y., Nishizawa, M., & Onodera, O. (2008). Soluble polyglutamine oligomers formed prior to inclusion body formation are cytotoxic. *Human Molecular Genetics*, *17*(3), 345–356. https://doi.org/10.1093/hmg/ddm311

Trottier, Y., Cancel, G., An-Gourfinkel, I., Lutz, Y., Weber, C., Brice, A., … Mandel, J.-L. (1998). Heterogeneous intracellular localization and expression of ataxin-3. *Neurobiology of Diseases*, *5*(5), 335–347. https://doi.org/10.1006/nbdi.1998.0208

Tsai, H. C., Su, H. L., Huang, C. Y., Fong, Y. C., Hsu, C. J., & Tang, C. H. (2014). CTGF increases matrix metalloproteinases expression and subsequently promotes tumor metastasis in human osteosarcoma through down-regulating miR-519d. *Oncotarget*, *5*(11), 3800–3812. https://doi.org/10.18632/oncotarget.1998

Türkmen, S., Guo, G., Garshasbi, M., Hoffmann, K., Alshalah, A. J., Mischung, C., … Robinson, P. N. (2009). CA8 mutations cause a novel syndrome characterized by ataxia and mild mental retardation with predisposition to quadrupedal gait. *PLoS Genetics*, *5*(5), e1000487. https://doi.org/10.1371/journal.pgen.1000487

Wang, K. K. (1990). Developing selective inhibitors of calpain. *Trends in Pharmacological Sciences*, *11*(4), 139–142. https://doi.org/10.1016/0165-6147(90)90060-L

Wang, T. K., Cheng, C. K., Chi, T. H., Ma, Y. S., Wu, S. B., Wei, Y. H., & Hsieh, M. (2014). Effects of carbonic anhydrase-related protein VIII on human cells harbouring an A8344G mitochondrial DNA mutation. *The Biochemical Journal*, *459*(1), 149–160. https://doi.org/10.1042/BJ20131235

Wang, T.-K., Lin, Y.-M., Lo, C.-M., Tang, C.-H., Teng, C.-L., Chao, W.-T., … Hsieh, M. (2016). Oncogenic roles of carbonic anhydrase 8 in human osteosarcoma cells. *Tumour Biology*, *37*(6), 7989–8005. https://doi.org/10.1007/s13277-015-4661-y

Wen, F.-C., Li, Y.-H., Tsai, H.-F., Lin, C.-H., Li, C., Liu, C.-S., … Hsieh, M. (2003). Down-regulation of heat shock protein 27 in neuronal cells and non-neuronal cells expressing mutant ataxin-3. *FEBS Letters*, *546*(2–3), 307–314. https://doi.org/10.1016/S0014-5793(03)00605-7

Yu, Y. C., Kuo, C. L., Cheng, W. L., Liu, C. S., & Hsieh, M. (2009). Decreased antioxidant enzyme activity and increased mitochondrial DNA damage in cellular models of Machado–Joseph disease. *Journal of Neuroscience Research*, *87*(8), 1884–1891. https://doi.org/10.1002/jnr.22011

SUPPORTING INFORMATION

Additional supporting information may be found online in the Supporting Information section at the end of the article.

Transparent Science Questionnaire for Authors.

How to cite this article: Hsieh M, Hsieh BY, Ma C-Y, Li Y-T, Liu C-S, Lo C-M. Protective roles of carbonic anhydrase 8 in Machado–Joseph Disease. *J Neuro Res*. 2019;97:1278–1297. https://doi.org/10.1002/jnr.24474